P516303.PDF [Page: 3 of 70]

Copy No. 12

DEFENCE R&D DÉFENSE

OPTIMIZATION OF VIBRATION MOUNT PROPERTIES FOR APPLICATION TO SHIPBOARD DIESEL ENGINES - PHASE III

S.G. Hutton

VIBE-TEK RESEARCH LTD.
5662 Holland Street
Vancouver
British Columbia
Canada
V6N 2A8

Defence R&D Canada

DEFENCE RESEARCH ESTABLISHMENT ATLANTIC

Contractor Report

DREA CR 2000-077

January 2001

National Defence Défense nationale

Canada

P516303.PDF [Page: 4 of 70]

104-06265/

Copy No: _____

OPTIMIZATION OF VIBRATION MOUNT PROPERTIES FOR APPLICATION TO SHIPBOARD DIESEL ENGINES - PHASE III

S.G. Hutton
VIBE-TEK RESEARCH LTD.
5662 Holland Street
Vancouver, British Columbia, Canada, V6N 2A8

Contract No: W7707-9-7025/001/HAL and W7707-9-7293/001/HAL

The scientific or technical validity of this Contract Report is entirely the responsibility of the contractor and the contents do not necessarily have the approval or endorsement of Defence R&D Canada.

Defence Research Establishment Atlantic

Contractor Report

DREA CR 2000-077

January 2001

Contract Scientific Authorities

D.C. Stredulinsky J. P. Szabo N.C. Sponagle

Approved by

J.L. Kennedy

Head, Warship Signatures & Safety

Approved for release by

Kirk Foster

Chair/DRP

© Her Majesty the Queen as represented by the Minister of National Defence, 2001

© Sa majesté la reine, représentée par le ministre de la Défense nationale, 2001

P516303.PDF [Page: 6 of 70]

Abstract

This report describes the theory and capabilities of MATLAB programs that have been developed in order to assist in the optimal vibration design of isolators for marine engines. These programs calculate the vibration transmissibility characteristics of the system and are of value in the design of optimal isolation systems. A program is also developed for the analysis of the active control of transmitted vibrations. The frequency range of interest is that encompassing the natural frequencies of the engine on its support system.

The general system that is analysed consists of an engine supported by vibration isolators on a foundation raft that itself is supported to ground by vibration isolators. The programs model the engine as a rigid body. The foundation raft can be modeled as a rigid body, or it can be modeled as a flexible body using beam finite elements. It is assumed that the isolators can be modeled as an isotropic linear viscoelastic material in terms of both a complex Young's modulus and a complex Poisson's Ratio, both of which are frequency dependant.

The report describes three different approaches to the modeling of the isolators: i) an approach based upon finite element analysis of the viscoelastic isolators using constitutive data of the isolator material; ii) an approach based upon the determination of the constitutive data from the results of dynamic stiffness measurements conducted on engine mounts; and iii) an approach based upon the results of so called 4-pole parameter data that describes the velocity force transfer matrices measured on full sized mounts in a given direction. In both the cases that involve experimentally determined isolator characteristics the data measured is not likely to completely describe the isolator characteristics. In such cases the programs developed have utilized an analytical approach to provide the missing data. In this way improved modeling of the actual structure is likely to occur. Numerical results are presented to illustrate each of the approaches developed.

A numerical problem that can occur in the finite element analysis of materials that are highly incompressible (as is the case with elastomeric materials used in vibration isolators) is described. A formulation is presented that avoids this problem.

The report also contains the development of an active control option which is used to evaluate the potential for active control to be used in order to minimise the levels of force transmitted from the engine to the support.

P516303.PDF [Page: 7 of 70]

Résumé

Le présent rapport décrit les principes et les capacités des programmes MATLAB qui ont été élaborés dans le but d'aider à la conception optimale des isolateurs de vibrations pour moteurs marins. Ces programmes établissent les caractéristiques de transmissibilité des vibrations du système et ils sont précieux pour la conception de systèmes d'isolation optimaux. Un programme est aussi élaboré pour l'analyse de la réduction active des vibrations transmises. La plage de fréquences d'intérêt est celle qui englobe les fréquences naturelles du moteur sur son support.

Le système général qui est analysé consiste en un moteur reposant sur des isolateurs de vibrations montés sur un radier, lequel prend appui au sol par l'intermédiaire d'autres isolateurs de vibrations. Les programmes modélisent le moteur comme étant un corps rigide. Le radier peut être modélisé comme un corps rigide, ou comme un corps flexible à l'aide d'éléments finis de poutre. On suppose que les isolateurs peuvent être modélisés comme un matériau viscoélastique linéaire isotrope en considérant un module de Young complexe et un coefficient de Poisson complexe, qui dépendent tous deux de la fréquence.

Le rapport décrit trois méthodes différentes de modélisation des isolateurs : i) une méthode basée sur l'analyse par éléments finis des isolateurs viscoélastiques faisant appel à des données constitutives du matériau de l'isolateur; ii) une méthode basée sur la détermination des données constitutives à partir des mesures de rigidité dynamique effectuées sur des supports de moteurs; iii) une méthode basée sur les données paramétriques dites quadripolaires qui décrivent les matrices de conversion de la vitesse en force établies pour des supports en grandeur réelle dans une direction donnée. Dans les deux méthodes basées sur les caractéristiques des isolateurs déterminées de façon expérimentale, les données obtenues ne semblent pas décrire complètement les caractéristiques des isolateurs. On a alors utilisé, dans les programmes élaborés, une méthode analytique permettant d'obtenir les données manquantes. On a ainsi des chances d'améliorer la modélisation de la structure réelle. Des résultats numériques sont présentés pour illustrer chacune des méthodes élaborées.

On décrit un problème numérique qui peut se poser dans l'analyse par éléments finis de matériaux hautement incompressibles (par exemple les élastomères utilisés dans les isolateurs de vibrations). On présente une façon de contourner ce problème.

Le rapport traite aussi de l'élaboration d'une option de réduction active utilisée pour évaluer les possibilités de réduction active en vue de minimiser les niveaux de la force transmise du moteur au support.

P516303.PDF [Page: 8 of 70]

Executive summary

Background

Marine diesel engines are supported by mounts that are designed to provide both structural rigidity and vibration isolation. Structural rigidity is required in order to maintain alignment of connecting shafts and piping; and vibration isolation is required in order to minimize the vibrations generated by the engine from being transmitted to the rest of the vessel and beyond. The vibration isolation materials currently in service on Canadian vessels, natural rubber and chloroprene rubber, experience large changes in their mechanical properties when exposed to lubricating oil or fuel. Replacing these materials with alternative elastomers could prevent alignment problems due to mount degradation, as well as reduce maintenance costs by increasing the length of time between mount changes. Replacement mounts must have a higher resistance to hydrocarbons and they must provide optimal vibration isolation. The optimal design of such mounts from a vibration viewpoint is complicated by the complex constitutive characteristics of the elastomers used in the construction of the mounts, and also by the complex nature of the three-dimensional vibration motion of the engine.

Principal Results

The principal result arising from this work is the further development of a computer program that enables the full three-dimensional vibration behaviour of a diesel engine mounted on polymeric isolators to be analyzed. The modeling capability of the program with respect to the engine support system has been extended. The program now has the ability to model an engine supported by an independent foundation raft, which is itself supported by ground. The isolators can be modeled on the basis of the geometric and constitutive properties of the isolator or they can be modeled on the basis of test results conducted on full-scale isolators. The program's capability has been extended to enable the modeling of isolators that have both complex Young's Modulus and complex Poisson's Ratio. An active control program has been implemented as an integral part of the VVES program and this will be used to investigate the possibilities of implementing active control of the engine transmitted vibrations.

Significance of Results

i) A sophisticated computational tool has been developed that will be of value in the optimal design of new isolators for marine diesel engines.

ii) An active control program has been developed that will assist in the evaluation of the future role of active control of engine vibrations.

Hutton, S.G. 2000. Optimization of Vibration Mount Properties For Application To Shipboard Diesel Engines - PHASE III. CR 2000-077 Defence Research Establishment Atlantic.

P516303.PDF [Page: 9 of 70]

Sommaire

Renseignements généraux

Les moteurs diesel marins ont des supports qui sont conçus pour assurer la rigidité structurale et un amortissement des vibrations. La rigidité structurale est essentielle au maintien de l'alignement des arbres et de la tuyauterie. L'amortissement des vibrations est requise pour réduire au minimum la transmission des vibrations produites par le moteur au reste du navire et au-delà. L'huile de graissage et les carburants influent beaucoup sur les propriétés mécaniques des matériaux utilisés actuellement à bord des navires canadiens pour amortir les vibrations, le caoutchouc naturel et le polychloroprène. Si ces matériaux étaient remplacés par d'autres élastomères, cela pourrait prévenir les problèmes d'alignement causés par la détérioration des supports et réduire les coûts d'entretien en réduisant la fréquence de remplacement des supports. Les supports de rechange doivent avoir une meilleure résistance aux hydrocarbures et doivent fournir un amortissement optimal des vibrations. La conception de ces supports, du point de vue des vibrations, est compliquée par les caractéristiques constitutives complexes des élastomères utilisés pour la fabrication des supports et par la nature complexe des mouvements vibratoires tridimensionnels du moteur.

Principaux résultats

Le principal résultat qui ressort de ces travaux est l'élaboration d'un programme informatique permettant d'analyser le comportement vibratoire tridimensionnel d'un moteur diesel placé sur des isolateurs en polymère. La capacité de modélisation du programme relativement au système de support de moteur a été augmentée. Le programme peut maintenant modéliser un moteur supporté par un radier indépendant qui est fixé à la structure du navire. Les isolateurs peuvent être modélisés en fonction des propriétés géométriques et constitutives de l'isolateur ou peuvent être modélisés en fonction des résultats des essais effectués sur des isolateurs de grandeur réelle. La capacité du programme a été augmentée pour permettre la modélisation d'isolateurs ayant un module de Young complexe et un coefficient de Poisson complexe. Un programme de contrôle actif a été intégré au programme VVES et sera utilisé pour étudier la possibilité d'appliquer un contrôle actif des vibrations transmises par le moteur.

Importance des résultats

i) Un outil de calcul complexe a été mis au point pour aider à la conception optimale de nouveaux isolateurs pour les moteurs diesel marins.

ii) Un programme de contrôle actif a été élaboré afin d'aider à l'évaluation du rôle futur du contrôle actif sur les vibrations de moteur.

Hutton, S.G. 2000. Optimisation des Propriétés des Supports Élastiques Utilisés sur les Moteurs Diesel de Navires – Étape III. CR 2000-077 Defence Research Establishment Atlantic.

P516303.PDF [Page: 10 of 70]

TABLE OF CONTENTS

	Page Number
Abstract	(i)
Résumé	(ii)
Executive Summary	(iii)
French Executive Summary	(iv)
Table of Contents	(v)
1. Introduction	1
2. Finite Element Analysis of the Isolators	3
2.1 Numerical examples	4
3. Analysis of Two Layer Isolation System	8
3.1 Modeling foundation raft as a flexible body	8
3.2 Modeling the foundation raft as a rigid body	8
3.3 Modeling of the Engine	8
4. Incorporation of Complex Young's Modulus and Complex Poisson's Ratio	9
5. Modeling of the Isolators	10
5.1 Finite Element Analysis (VVESANALYSIS.m)	10
5.1.1 Numerical Results	10
5.2 Measured Dynamic Stiffness (VVESDYNSTFF.m)	12
5.2.1 Basic Theory	12
5.2.2 Numerical Results	13
5.3 Four-Pole Parameter Data Input (VVES4POLE.m)	15
5.3.1 Basic Theory	15
5.3.2 Some Simple Systems	16
5.3.2.1 Four-Pole Representations	17
5.3.2.2 Dynamic Stiffness Representation	17
5.3.3 Theoretical Development of General Transmissibility Matrix	18
5.3.4 General Transmissibility Matrix from Measured Four-Pole Data	20
5.3.5 Parallel Assemblies of Isolators	21
5.3.6 Equations Governing Transmission Characteristics of Complete System	24
5.3.7 Numerical Results	26
6. Active Control of Transmitted Vibrations	32
6.1 Introduction	32
6.2 Feedforward Adaptive Control	32
6.3 Multi-Channel Feedforward Adaptive Control	36

P516303.PDF [Page: 11 of 70]

TABLE OF CONTENTS (cont)

	Page Number
6.4 Multi-Channel Feedforward Adaptive Control with a Displacement Reference Sensor	38
7. Summary	41
8. References	43
Appendix 1 Finite Element Modeling of Isolators	44
Appendix 2 Effect of Complex Poisson's Ratio on Condensation Procedure	50

OPTIMIZATION OF VIBRATION ISOLATION MOUNT PROPERTIES FOR APPLICATION TO SHIP BOARD ENGINES – PHASE III

1. Introduction

In a previous contract [1] a MATLAB based computer program VVES10 was developed to predict the vibration response characteristics of a marine diesel engine when supported on elastomeric vibration isolators that were themselves supported on elastic beams. This program determined the properties of the isolators by assuming that complex constitutive data was available for Young's Modulus and that Poisson's Ratio was real.

In the present contract this program is further developed and a numerical problem that occurred for isolators that were highly incompressible has been rectified. Modeling of the basic system is extended to include:

- A rigid, or flexible, engine foundation support raft with isolators between the engine and the raft and also between the raft and ground.
- The ability to model the isolators as either rectangular blocks or as solid or hollow cylinders or cones.
- The ability to input the viscoelastic characteristics of the isolators in terms of both complex Young's Modulus and complex Poisson's ratio.
- The ability to input measured complex stiffness data for the isolators directly into the program.
- The ability to use measured, so called, four-pole parameter data in combination with analytically derived properties to predict the transmissibility characteristics of the system.

Also included in this report is a description of software that has been developed in order to examine the possibility of active control of the vibrations transmitted from the engine to the support structure as result of the unbalanced excitation that occurs in low speed diesel engines.

The following assumptions are made in the analysis developed in this report:

i) the engine can be modeled as a rigid body

ii) the foundation raft can be modeled either by elastic finite element beam elements or as a rigid body with prescribed geometric and inertial characteristics

iii) the isolators can be modeled in a number of different ways:

a) by analysis of a viscoelastic isotropic material whose frequency dependant constitutive characteristics are known;

b) in terms of analysis based upon measured complex stiffness data; or

c) in terms of measured four pole parameter data supplemented by analysis.

iv) the region of contact between the isolator and the engine/raft/support is considered to be locally rigid i.e. the deformation of the contact surface between the isolator and the engine and its supports can be completely defined by three displacements and three rotations. This assumption allows each isolator to be represented in terms of stiffness and mass matrices of size (12x12).

P516303.PDF [Page: 13 of 70]

The resulting predictions are therefore limited by these assumptions. In the actual situation there will also be local vibration modes associated with items such as the engine enclosure and the attached piping and shafting. Such issues are not considered in the present model. The foundation raft will normally be very stiff and its natural frequencies much higher than those of the engine on the isolators. In such cases the raft can be modeled as a rigid body and this capability has been added to the program. However in order to assess the effects of raft flexibility the program developed also allows for the raft to be idealised in terms of beam finite elements and thus its frequency characteristics can be included in the analysis

The program developed has been designed to be used to investigate the low frequency vibration transmission characteristics of an engine and its support system in the frequency range of the engine and its first harmonic. Of particular interest is the ability to model the full three dimensional behaviour of the engine and raft, together with the ability to analyse the effect of different isolators upon the levels of transmitted vibration.

P516303.PDF [Page: 14 of 70]

2. Finite element analysis of the isolators

The engine isolators that are used in marine applications are fabricated from elastomeric materials whose constitutive relations cannot be accurately modeled as linearly elastic. A more realistic representation of their vibration behaviour is obtained by modeling them in terms of a linear viscoelastic material.

Many elastomeric materials of the type used for isolators have the property that they are almost incompressible. This is reflected by the fact that the value of Poisson's Ratio is close to 0.5 (a completely incompressible material has an infinite bulk modulus K where K = E/3*(1-2*v) and E = Young's Modulus, v = Poisson's Ratio). In such circumstances small errors in the calculation of the volumetric change, which depends upon the derivative of the predicted displacements, can lead to large errors in the predicted stresses when using a pure displacement based finite element formulation. This stress error will, in turn, effect the displacement prediction, as the applied load will not be correctly balanced due to the error in the stresses. The usual solution to this problem is to use a mixed finite element formulation in which both the pressure and the displacements are treated as independent unknowns [2]. Such an approach has been adopted in the present contract.

Two types of solid finite elements are used in order to model the isolator shapes. They are a 20- node parabolic solid and a 15- node parabolic wedge element with both these elements having a mixed displacement pressure formulation. (In the previous contract 8 node solid elements were used with a pure displacement formulation.) For the elements developed the pressure distribution is linear in each element. These two elements enable a wide range of isolator shapes (including those with curved boundaries) to be modeled as shown in Figure 1. The development of the required stiffness matrices are presented in Appendix 1

The isolator's stiffness characteristics are modeled using viscoelastic material properties. These may be input into the program by means of a Rational Polynomial (RP) representation or in terms of a Havrilak-Negami (HN) representation, or they may be input directly by means of a table listing the real and imaginary parts of the complex moduli required for the analysis. A description of these representations can be found in the users manual.

The analysis of the effect of the isolators on the system response is conducted on the basis of a condensed representation of each isolator. This is done in order to minimize the size of the analysis problem. Each isolator type is modeled to the required degree of accuracy using three dimensional isoparametric brick finite elements and then a condensation procedure is used to reduce the mass and stiffness matrices to a 12x12 size. Thus the connectivity between the isolator and the engine/raft/support is reduced to one having six degrees of freedom (three displacements and three rotations). This condensation is based upon the assumption that the both the top and bottom surfaces of the isolator remain planar during deformation. Given the relatively small footprint of each isolator pad this assumption appears to be reasonable in the frequency range of interest. A result of the condensation used is that the program will not predict internal isolator resonances which occur at frequencies well above the engine frequencies considered in this study.

P516303.PDF [Page: 15 of 70]

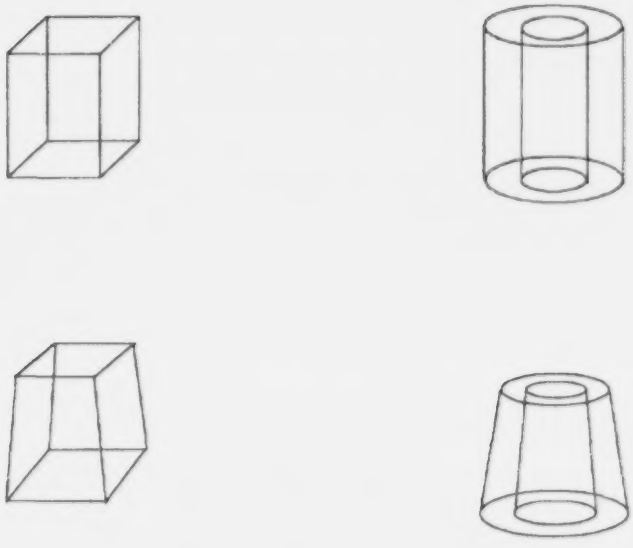

Figure.1 Available Isolator Shapes

During idealisation of the complete system, in order to best represent the total geometry of the system, it will sometimes be necessary for the isolator element length used to be somewhat different to its actual length. For example, when using a flexible raft model (and therefore using beams that are modeled by the position of their centre lines) it will often be necessary for the condensed element length to be different to the actual length of the isolator.

The analysis assumes that the engine (and perhaps the raft) is rigid. From this assumption follows the fact that the deformation of every isolator support point can be defined in terms of the three displacements and three rotations of the centre of mass and the geometry of the engine (or the raft). In this way all the degrees of freedom defining the deformation of the engine (raft) support locations can be eliminated from the problem.

2.1 Numerical Examples

In the previous contract an 8 node pure displacement solid brick finite element was used to model the isolator. In the present contract this element has been replaced with a mixed element formulation that consists of a 20 node displacement element together with a linear pressure assumption. The theory governing this formulation is presented in Appendix 1. Table 1 presents a comparison of the results given by different elements for the displacement of a unit cube fixed on one face with a uniformly distributed force of total magnitude 1 applied on the opposite face. It is assumed that the

P516303.PDF [Page: 16 of 70]

Young's Modulus is 1.e6 and the effect of Poisson's Ratio approaching 0.5 is investigated. For the case where Poisson's Ratio is zero the exact result is 1.e-6. In Table 1 the U-mode refers to the pure displacement formulation and the UP mode refers to the mixed pressure-displacement formulation. As may be noted Nastran refuses to conduct the analysis when Poisson's Ratio reaches a value of .499995.

Poisson's Ratio	4x4x8 Nastran (8 Node)	2 x 2 x4 U-mode	4 x 4 x 8 U-mode	1 x 1 x 2 UP-mode	2 x 2 x 4 UP-mode	4 x 4 x 8 UP-mode
0	1e-6	1e-6	1e-6	1e-6	1e-6	1e-6
0.45	9.2604e-7	8.6745e-7	9.0298e-7	9.0153e-7	9.1107e-7	9.1987e-7
0.495	9.0466e-7	5.9124e-7	7.7272e-7	8.7830e-7	8.8904e-7	8.9919e-7
0.4995	9.0230e-7	1.5700e-7	3.9938e-7	8.7580e-7	8.8664e-7	8.9692e-7
0.49995	9.0213e-7	1.8796e-8	7.0458e-8	8.7555e-7	8.8640e-7	8.9669e-7
0.499995	No result	1.9159e-9	7.6142e-9	8.7553e-7	8.8638e-7	8.9667e-7
0.49999999995	No result	1.9200e-15	7.6800e-15	8.7553e-7	8.8637e-7	8.9666e-7

Table 1 Comparison of Results Using 8-Node Elements

As may be seen from these results the pure displacement formulation (which was used in the previous contract) produces increasingly inaccurate answers as Poisson's Ratio approaches .5. The mixed pressure formulation can be seen to perform much better. In the present contract however, it was decided that better modeling capabilities could be obtained, especially for curved boundaries, by the use of a 20 node displacement formulation in conjunction with a linear pressure assumption. The results of using the 20 node element on this same problem are presented in Table 2.

Poisson's Ratio	4x4x8 Nastran (27 Node)	2 x 2 x4 U-mode	4 x 4 x 8 U-mode	1 x 1 x 2 UP-mode	2 x 2 x 4 UP-mode	4 x 4 x 8 UP-mode
0	1e-6	1e-6	1e-6	1e-6	1e-6	1e-6
0.45	9.3130e-7	9.1399e-7	9.2120e-7	8.8566e-7	9.3762e-7	9.3321e-7
0.495	9.0722e-7	8.8179e-7	8.9689e-7	8.6323e-7	9.2266e-7	9.1494e-7
0.4995	9.0245e-7	8.7307e-7	8.9210e-7	8.6088e-7	9.2105e-7	9.1476e-7
0.49995	9.0137e-7	8.7063e-7	8.9093e-7	8.6065e-7	9.2089e-7	9.1476e-7
0.499995	No result	8.6969e-7	8.9093e-7	8.6062e-7	9.2087e-7	9.1474e-7
0.499999999995	No result	8.6914e-7	8.8922e-7	8.6063e-7	9.2089e-7	9.1457e-7

Table 2 Comparison of Results Using 20-Node Elements

As may be noted the results from the 20 node pure displacement element do not appear to be adversely affected as Poisson's Ratio approaches .5. However the mixed linear pressure and 20 node displacement element has been incorporated into the code.

P516303.PDF [Page: 17 of 70]

A further numerical comparison was made by considering the analysis of an isolator rigidly connected to a top rigid mass. The isolator was fixed at its base and the rigid mass was unconstrained. A force of magnitude 1000 was applied in horizontal (x) and vertical (z) directions to the node at the centre of the isolator/top mass interface. A comparison was made of the resulting maximum displacements in the x direction (u) and in the vertical direction (w). Note that a horizontal force produces both lateral and vertical motion due to the rigid body rotation of the top mass.

The isolator dimensions were: 0.15m x 0.15m x 0.054m (x=0.15; y=0.15; z=0.054); E=1e3, Density =1e3. The rigid top mass dimensions were:0.15m x 0.15m x 0.046m; its properties were those of steel. The isolator and rigid top have a common surface with all nodes connected at the interface. The base of the isolator is fully fixed to ground. The results are given in Table 3 in which the U-Mode refers to the pure displacement formulation using 20 node elements and the UP mode refers to the displacement pressure formulation using 20 node displacement elements and a linear pressure distribution.

Poisson's Ratio	Load		Nastran (27 node) 6x6x6	U-Mode 4x4x4	U-Mode 6x6x6	UP-Mode 4x4x4	UP-Mode 6x6x6
0.0	Fx=1000	U	6.529	6.4993	6.5794	6.655	6.6127
		W	2.592	2.5920	2.5920	2.6723	2.6275
	Fz=1000	W	2.400	2.4000	2.4000	2.4000	2.4000
0.3	Fx=1000	U	7.828	7.7642	7.8256	8.0613	7.9846
		W	2.293	2.2814	2.2919	2.3936	2.3484
	Fz=1000	W	2.041	2.0170	2.0423	2.0519	2.0458
0.4	Fx=1000	U	8.126	8.0273	8.1209	8.4304	8.3399
		W	2.016	1.9937	2.0143	2.1456	2.0988
	Fz=1000	W	1.655	1.6400	1.6541	1.7270	1.7084
0.49	Fx=1000	U	8.223	8.0456	8.2153	8.7001	8.5940
		W	1.629	1.5858	1.6271	1.8291	1.7784
	Fz=1000	W	1.113	1.0886	1.1114	1.2850	1.2374
0.499	Fx=1000	U	8.171	7.9848	8.1639	8.7230	8.6150
		W	1.565	1.5052	1.5630	1.7889	1.7357
	Fz=1000	W	1.032	0.9945	1.0307	1.2298	1.1774

Table 3 Comparison of Static Displacements of Isolator with Rigid Top Mass

As may be seen the Nastran results using a 27 node element agree very closely with the U-mode results, obtained with 20 node elements. The UP results are also in good agreement.

These numerical tests indicate that the pure displacement formulation gives the same results as Nastran as would be expected. It would appear that either the 20 node pure displacement element or the mixed pressure-displacement formulation could be used. It was decided to use the mixed formulation.

As a further test a comparison was made between the natural frequencies predicted by an uncondensed Nastran model and a condensed VVES20 model. The example consisted of two single isolators and two rigid masses. The isolators were of size 0.15 x 0.15.x 0.054 with E=1e6 and density =1; and the rigid masses were of size 0.15 x 0.15 x 0.046 with E=1e12 and density 1e6. In the Nastran model each component was modeled with 4x4x4 27 node elements. In the VVES20 model the isolators were modeled with 4x4x4 20 node mixed formulation elements. The results are given in Table 4.

Mode Number	Poisson's Ratio = 0.30		Poisson's Ratio = 0.499	
	Nastran	VVES20	Nastran	VVES20
1	0.684	0.6847	0.769	0.7542
2	0.684	0.6847	0.769	0.7542
3	1.152	1.1248	1.101	1.0585
4	2.152	2.1501	2.377	2.3469
5	2.297	2.3088	2.377	2.3469
6	2.297	2.3088	2.881	2.7713
7	3.016	2.9448	3.064	2.9747
8	4.066	4.1219	4.143	4.1426
9	4.066	4.1219	4.143	4.1426
10	5.540	5.6290	6.597	6.6048

Table 4 Comparison of Predicted Natural Frequencies

As may be seen the agreement is very good and indicates that the condensation procedure is working well.

P516303.PDF [Page: 19 of 70]

3. Analysis of two stage isolation systems.

It is common practice in the design of isolation systems for marine engines to use a two-stage isolation system. In such a system the engine is connected to a foundation raft by elastomeric isolators and the foundation raft itself is isolated from the hull of the ship by a second set of isolators. In the calculation of high frequency response characteristics the vibration characteristics of the raft need to be considered whereas for low frequency predictions it will be possible to treat the raft as a rigid body. The present program has been developed such that the foundation raft can be modeled as a rigid body or as a flexible assembly of beams. It should be noted that in the present model any dynamics of the hull are neglected.

In the programs developed in this contract it is possible to analyse such two stage isolator systems. Different isolators can have different material characteristics whereas in the previous version of the program VVES10 it was assumed that all the isolators had the same material characteristics.

3.1 Modeling of the foundation raft as a flexible body

The foundation raft is modeled as an assembly of beam finite elements. It is not the intention that this capability will be used to attempt to model in detail an actual foundation raft. Rather it provides a convenient tool to investigate the effect that different raft natural frequencies and mode shapes may have on the transmission characteristics of the isolation system.

In this modeling approach it is important to correctly account for the depth of the foundation raft beams by correctly defining the lengths of the condensed isolators in COORD.ext. This problem arises as the actual depth of the lower isolators will be between ground and the underside of the raft beams. However the modeling of the raft beams is conducted with finite elements along the neutral axis of the beams.

3.2 Modeling of the foundation raft as a rigid body

In this case the raft is characterised by its inertial properties (both mass and rotational inertia) contained in RAFT.ext and by its geometry defined by the nodal points of the isolators that are connected to the raft. In this modeling approach the condensed length of the isolators will be the same as their physical length. It is assumed that the principal inertial axes of the raft coincide with the global axes.

3.3 Modeling of the engine

The engine is modeled as a rigid body in terms of its inertial and geometric characteristics specified in ENGINE.ext. The nodal points of the isolators connected to the engine define its geometry. It is assumed that the principal inertial axes of the engine coincide with the global axes.

4. Incorporation of Complex Young's Modulus and Complex Poisson's Ratio

In the previous contract it had been assumed that the complex Poisson's Ratio operator of the isolator material could be assumed to be real. In this study that restriction is removed.

In the development of VVES10 it was assumed, for harmonic response, that Poisson's ratio was real which in effect means that the loss factor for the complex shear modulus and the loss factor for the complex Young's modulus were the same. In general this will not be true and the program is further generalised to include this fact. The mathematics required in this case to enable a consistent condensation of the isolator stiffness is complicated and is presented in Appendix 2.

5. Modeling of the Isolators

In the present contract a number of different approaches were developed in order to provide flexibility in the manner by which the behaviour of the isolators can be modeled. In this chapter these approaches are reviewed.

5.1 Finite Element Analysis (VVESANALYSIS.m)

In this approach, which was the one used in the previous contract, the properties of the isolators are determined by a finite element analysis that is based upon the geometry and constitutive data provided by the user. In the previous contract the isolators were modeled using finite element procedures with the assumption that Poisson's ratio was real. In the present contract that restriction has been removed and the analysis now is conducted on the basis that for harmonic excitation both Young's Modulus and Poisson's Ratio are complex. In this approach a detailed finite element analysis of the isolators are conducted and then a condensation procedure is used to reduce their stiffness matrix to a 12x12 size i.e. their stiffness characteristics are expressed in terms of equivalent one dimensional elements with six degrees of freedom at each node. These condensed stiffeners are then incorporated into a full three-dimensional analysis of the vibration response characteristics of the engine/mount/isolator system. The inertial characteristics of the isolators are assumed to be negligible compared to those of the engine and the raft.

The program that results from this approach is now called VVESANALYSIS.m and its predictions are based upon a knowledge of the constitutive properties of the isolator mount and the assumption that these properties can be modeled as an isotropic linear viscoelastic continuum. In this program each of the isolators can have different geometric or constitutive properties.

5.1.1 Numerical Results.

A representative example was chosen in order to compare the numerical predictions of the various programs. The data for this example is given in the User Manual. The results obtained from VVESANALYSIS.m for this case are listed in Table 5

Mode	Frequency (Hz)	Mode Shape
1	-.01898 + i1.8339	Engine Ty motion (Translation in Y direction. Engine and raft move in the same direction
2	-.02200 +i2.0122	Engine Tx motion (translation in X direction). Engine and raft move in the same direction
3	-.05781 +i3.5338	Engine Rz rotation (rotation about Z direction). Engine and raft rotate in the same direction
4	-.1462 +i5.1446	Engine Tz motion (bounce mode). Engine and raft move in the same direction
5	-.2285 +i6.2196	Engine Rx rotation. Engine and raft move in the same direction
6	-.2029 +i6.3337	Engine Ry rotation. Engine and raft move in the same direction
7	-.3406 +i9.7404	Tx motion. Engine and raft move in the opposite Direction
8	-.4565 +i11.672	Ty motion. Engine and raft move in the opposite Direction
9	-.1905 +i19.372	Raft Rz rotation. Engine stationary
10	-.1638 +i19.868	Raft Tz motion. Engine almost stationary
11	-.9139 +i41.154	Raft Ry rotation. Engine stationary
12	-.8246 +i43.15	Raft Rx rotation. Engine stationary

Table 5 Natural Frequencies and Mode Shapes Predicted by VVESANALYSIS.m

5.2 Measured Dynamic Stiffness (VVESDYNSTFF.m)

An alternative approach to the determination of the stiffness characteristics of the isolators is to conduct full- scale tests upon the isolators themselves. Such tests could result in, for example, complex values of dynamic axial stiffness plus complex values of dynamic shear stiffness in two orthogonal directions. A special program has been developed to enable such data to be used in the analysis of overall engine/raft response. This program is called VVESDYNSTFF.m.

5.2.1 Basic theory

In the previous program VVESANALYSIS.m the element dynamic stiffness matrix of isolators was obtained in terms of a 12x12 matrix as follows:

$$\mathbf{Z}_v(\omega) = G_1(\omega)\mathbf{K}_{v1} + G_2(\omega)\mathbf{K}_{v2} - \omega^2\rho\mathbf{M}_v$$

where $\mathbf{K}_{v1}$, $\mathbf{K}_{v2}$ and $\mathbf{M}_v$ are only dependant upon the geometric shape of the isolator and are calculated on the basis of a finite element analysis.
For the case where the dynamic stiffness is input directly the values of $G_1(\omega)$ and $G_2(\omega)$ can be evaluated from the input data. For example the element matrix components $(\mathbf{Z}_v)_{11}$, $(\mathbf{Z}_v)_{22}$, and $(\mathbf{Z}_v)_{33}$ may be input directly on the basis of experimental tests.
Define:

$k_1(\omega_j) = (\mathbf{Z}_v)_{11}(\omega_j)$

$k_2(\omega_j) = (\mathbf{Z}_v)_{22}(\omega_j)$

$k_3(\omega_j) = (\mathbf{Z}_v)_{33}(\omega_j)$

Prediction of the response characteristics of the engine/raft/isolator system could be conducted on the assumption that these three dynamic stiffnesses constituted the total stiffness of the isolator i.e. all rotational and coupling effects are neglected. However a better approach is to use the measured data in order to compute the complex constitutive constants $G_1(\omega_j)$ and $G_2(\omega_j)$ and then calculate the remaining components of the dynamic stiffness matrix using this data.
Thus: $G_1(\omega_j)$ and $G_2(\omega_j)$ can be solved from the following equations

$$G_1(\omega_j)(\mathbf{K}_{v1})_{11} + G_2(\omega_j)(\mathbf{K}_{v2})_{11} = k_1(\omega_j) + \omega_j^2\rho(\mathbf{M}_v)_{11}$$

$$G_1(\omega_j)(\mathbf{K}_{v1})_{22} + G_2(\omega_j)(\mathbf{K}_{v2})_{22} = k_2(\omega_j) + \omega_j^2\rho(\mathbf{M}_v)_{22}$$

$$G_1(\omega_j)(\mathbf{K}_{v1})_{33} + G_2(\omega_j)(\mathbf{K}_{v2})_{33} = k_3(\omega_j) + \omega_j^2\rho(\mathbf{M}_v)_{33}$$

solving for $G_1(\omega_j)$ and $G_2(\omega_j)$ gives:

$$\begin{Bmatrix} G_1(\omega_j) \\ G_2(\omega_j) \end{Bmatrix} = (\mathbf{A}^T\mathbf{A})^{-1}\mathbf{A}^T\mathbf{B}$$

where

$$\mathbf{A} = \begin{bmatrix} (\mathbf{K}_{v1})_{11} & (\mathbf{K}_{v2})_{11} \\ (\mathbf{K}_{v1})_{22} & (\mathbf{K}_{v2})_{22} \\ (\mathbf{K}_{v1})_{33} & (\mathbf{K}_{v2})_{33} \end{bmatrix} \qquad \mathbf{B} = \begin{Bmatrix} k_1(\omega_j) + \omega_j^2 \rho(\mathbf{M}_v)_{11} \\ k_2(\omega_j) + \omega_j^2 \rho(\mathbf{M}_v)_{22} \\ k_3(\omega_j) + \omega_j^2 \rho(\mathbf{M}_v)_{33} \end{Bmatrix}$$

The complete element viscoelastic matrix is then:

$$\mathbf{Z}_v(\omega_j) = G_1(\omega_j)\mathbf{K}_{v1} + G_2(\omega_j)\mathbf{K}_{v2} - \omega^2\mathbf{M}_v$$

At this stage the complete 12x12 dynamic stiffness is available and the analysis of the resulting response follows the same path as in VVESANALYSIS.m. In VVESDYNSTFF.m it is assumed that each layer is composed of isolators that have the same properties. The properties may vary between the layers.

5.2.2 Numerical Results

In order to check the performance of VVESDYNSTFF.m artificial dynamic stiffness data was created using the equations of motion that form the basis of the program VVESANALYSIS. Thus the dynamic stiffness data was computed for the response of the isolators (.2x.4x.2m) in the x, y, and z directions due to harmonic forces in these same directions. Motion was only permitted for the degree of freedom being measured i.e. the diagonal elements of the dynamic stiffness matrix were measured. This data was input into DIRECTSTIFF.ext and the program VVESDYNSTFF.m run. The resulting natural frequencies are listed in Table 6. These results may be compared with the corresponding results in Table 5 obtained by running VVESANALYSIS.m. As may be verified the predictions from the two programs are essentially the same.

Mode	Frequency (Hz)	**Mode Shape**
1	-.01897 +i1.8341	Engine Ty motion (Translation in Y direction. Engine and raft move in the same direction
2	-.02199 +i2.0124	Engine Tx motion (translation in X direction). Engine and raft move in the same direction
3	-.05776 +i3.5344	Engine Rz rotation (rotation about Z direction). Engine and raft rotate in the same direction
4	-.1459 +i5.1477	Engine Tz motion (bounce mode). Engine and raft move in the same direction
5	-.2279 +i6.2268	Engine Rx rotation. Engine and raft move in the same direction
6	-.2024 +i6.3388	Engine Ry rotation. Engine and raft move in the same direction
7	-.3386 +i9.7514	Tx motion. Engine and raft move in the opposite Direction
8	-.4528 +i11.689	Ty motion. Engine and raft move in the opposite Direction
9	-1.861 +i19.553	Raft Rz rotation. Engine stationary
10	-1.600 +i19.999	Raft Tz motion. Engine almost stationary
11	-8.278 +i42.819	Raft Ry rotation. Engine stationary
12	-7.4441 +i44.370	Raft Rx rotation. Engine stationary

Table 6 Natural Frequencies and Mode Shapes Predicted by VVESDYNSTFF

5.3 Four-Pole Parameter Data Input (VVES4POLE.m)

A different approach to the determination of the response of the complete system is that afforded by a transfer matrix approach. In this approach the global system is considered to consist of the following subsystems: i) the base; ii) the lower isolators grouped together; iii) the rigid raft; iv) the upper isolators grouped together; and v) the engine. Transfer function matrices are written for each of the components in terms of input and output velocities and forces and these are used sequentially to trace the value of these variables through the system.

This approach will be considered in this section. In the program developed it is assumed that each layer of isolators consists of isolators with the same properties. The properties may vary between the layers.

5.3.1 Basic Theory

Figure 1 represents graphically the relationship between input and output velocities and forces in a given direction for a general mechanical system subjected to harmonic excitation. The system may be comprised of one or more distributed elements, or be constructed from any combination of such elements. The input side of the system vibrates with a velocity $V_1 \exp(iwt)$ in response to an applied force $F_1 \exp(iwt)$. In turn the output side of the system exerts a force $F_2 \exp(iwt)$ on the input side of some further system, sharing with it a common velocity $V_2 \exp(iwt)$. In general V and F will be complex quantities.

Thus the system shown is said to have input and output terminal pairs which consist of a force F_1 and velocity V_1 at the input terminal giving rise to a force F_2 and a velocity V_2 at the output terminal, the reaction of any subsequent mechanical system being accounted for. Forces are considered positive when directed upward. Such a representation was used to analyze the behaviour of vibration isolator systems by Snowdon [3], and has been investigated further by Dickens and Norwood [4].

In this section the ideas that have been used in the context of the response of a mechanical system in one direction are generalized to account for the behaviour of a vibration isolator with twelve degrees of freedom or a collection of such isolators. In the case of response and excitation in one direction, the relationship between the forces and velocities can be expressed in the following form:

$$\begin{Bmatrix} F_1 \\ V_1 \end{Bmatrix} = \begin{bmatrix} a_{11} & a_{12} \\ a_{21} & a_{22} \end{bmatrix} \begin{Bmatrix} F_2 \\ V_2 \end{Bmatrix} \qquad (1)$$

The coefficient matrix in the above expression, which consists of four scalars, is known as a four-pole parameter matrix. Such a representation is valid when the input and the output are in the same direction. For more complicated systems, where the inputs and the outputs may be in a number of different directions, the inputs and the outputs can be expressed in vector form.

The input pairs and output pairs can then be specified to be $\mathbf{V}_1$, $\mathbf{F}_1$ and $\mathbf{V}_2$,

P516303.PDF [Page: 27 of 70]

$\mathbf{F}_2$ respectively. Then their relationship will have the form:

$$\begin{Bmatrix} \mathbf{F}_1 \\ \mathbf{V}_1 \end{Bmatrix} = \begin{bmatrix} \mathbf{a}_{11} & \mathbf{a}_{12} \\ \mathbf{a}_{21} & \mathbf{a}_{22} \end{bmatrix} \begin{Bmatrix} \mathbf{F}_2 \\ \mathbf{V}_2 \end{Bmatrix} = \mathbf{A} \begin{Bmatrix} \mathbf{F}_2 \\ \mathbf{V}_2 \end{Bmatrix} \tag{2}$$

where the elements of the coefficient matrix will themselves be matrices. An example of the above is that of a rigid body which requires three translational and three rotational degrees of freedom to specify its motion. Such a matrix is a generalization of the four-pole matrix and will be referred to as the transmissibility parameter matrix.

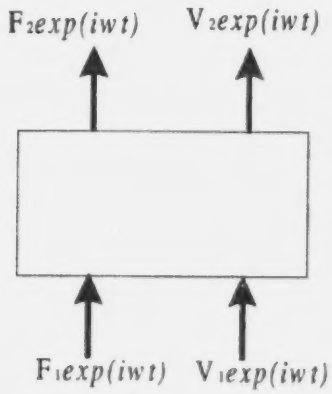

Figure 1 Four-Pole Parameter Representation of a Mechanical System

Further, for a series connection of such systems, there exists the following relation between the first input pair and the last output pair:

$$\begin{Bmatrix} \mathbf{F}_1 \\ \mathbf{V}_1 \end{Bmatrix} = \mathbf{A}_1\mathbf{A}_2\cdots\mathbf{A}_n \begin{Bmatrix} \mathbf{F}_{n+1} \\ \mathbf{V}_{n+1} \end{Bmatrix} \tag{3}$$

From this relationship, a force or velocity transmissibility function matrix can be determined for a wide class of problems including that of vibration isolation.

Experimental facilities exist for the determination of the four pole parameters for full sized isolators [4]. Such experimental data does not generally fully define the dynamic characteristics of the complete system. Of interest is the extent to which such data can be used to predict the behaviour of the engine/raft/isolator system.

5.3.2 Some Simple Systems

In this section the four-pole parameter and the equivalent dynamic stiffness representation of some simple systems will be presented. The four-pole representation is expressed in the form:

$$\begin{Bmatrix} F_1 \\ V_1 \end{Bmatrix} = \begin{bmatrix} a_{11} & a_{12} \\ a_{21} & a_{22} \end{bmatrix} \begin{Bmatrix} F_2 \\ V_2 \end{Bmatrix} \tag{4}$$

whereas the dynamic stiffness representation of the same system can be expressed in the form:

$$\begin{bmatrix} b_{11} & b_{12} \\ b_{21} & b_{22} \end{bmatrix} \begin{Bmatrix} V_1 \\ V_2 \end{Bmatrix} = \begin{Bmatrix} F_1 \\ -F_2 \end{Bmatrix} \tag{5}$$

where

$$\begin{bmatrix} b_{11} & b_{12} \\ b_{21} & b_{22} \end{bmatrix} = \begin{bmatrix} a_{11}a_{21}^{-1} & a_{12} - a_{11}a_{21}^{-1}a_{22} \\ -a_{21}^{-1} & a_{21}^{-1}a_{22} \end{bmatrix}$$

5.3.2.1 Four Pole Representation

For a mass m:

$$\begin{Bmatrix} F_1 \\ V_1 \end{Bmatrix} = \begin{bmatrix} 1 & i\omega m \\ 0 & 1 \end{bmatrix} \begin{Bmatrix} F_2 \\ V_2 \end{Bmatrix} = \mathbf{A}_m \begin{Bmatrix} F_2 \\ V_2 \end{Bmatrix} \tag{6}$$

For a spring with stiffness k:

$$\begin{Bmatrix} F_1 \\ V_1 \end{Bmatrix} = \begin{bmatrix} 1 & 0 \\ i\omega k^{-1} & 1 \end{bmatrix} \begin{Bmatrix} F_2 \\ V_2 \end{Bmatrix} = \mathbf{A}_k \begin{Bmatrix} F_2 \\ V_2 \end{Bmatrix} \tag{7}$$

For a dashpot of viscosity η:

$$\begin{Bmatrix} F_1 \\ V_1 \end{Bmatrix} = \begin{bmatrix} 1 & 0 \\ \eta^{-1} & 1 \end{bmatrix} \begin{Bmatrix} F_2 \\ V_2 \end{Bmatrix} = \mathbf{A}_\zeta \begin{Bmatrix} F_2 \\ V_2 \end{Bmatrix} \tag{8}$$

For parallel spring and dashpot:

$$\begin{Bmatrix} F_1 \\ V_1 \end{Bmatrix} = \begin{bmatrix} 1 & 0 \\ i\omega(k + i\omega\eta)^{-1} & 1 \end{bmatrix} \begin{Bmatrix} F_2 \\ V_2 \end{Bmatrix} = \mathbf{A}_{k\zeta} \begin{Bmatrix} F_2 \\ V_2 \end{Bmatrix} \tag{9}$$

For a single-degree of freedom system without damping:

$$\mathbf{A}_{km} = \mathbf{A}_k \mathbf{A}_m = \begin{bmatrix} 1 & i\omega m \\ \omega k^{-1} & 0 \end{bmatrix} \tag{10}$$

For a single-degree of freedom system with damping:

$$\mathbf{A}_{k\zeta m} = \mathbf{A}_{k\zeta} \mathbf{A}_m = \begin{bmatrix} 1 & i\omega m \\ i\omega(k + i\omega\eta)^{-1} & 1 - m\omega^2(k + i\omega\eta)^{-1} \end{bmatrix} \tag{11}$$

5.3.2.1 Dynamic Stiffness Matrix Representation

For a mass m:

$$i\omega \begin{bmatrix} m & 0 \\ 0 & m \end{bmatrix} \begin{Bmatrix} V_1 \\ V_2 \end{Bmatrix} = \begin{Bmatrix} F_1 - F_2 \\ F_1 - F_2 \end{Bmatrix} \tag{12}$$

P516303.PDF [Page: 29 of 70]

For a spring with stiffness k :

$$(i\omega)^{-1}\begin{bmatrix} k & -k \\ -k & k \end{bmatrix}\begin{Bmatrix} V_1 \\ V_2 \end{Bmatrix} = \begin{Bmatrix} F_1 \\ -F_2 \end{Bmatrix} \tag{13}$$

For a single-degree of freedom system with damping:

$$\left[i\omega\begin{bmatrix} 0 & 0 \\ 0 & m \end{bmatrix} + \begin{bmatrix} \eta & -\eta \\ -\eta & \eta \end{bmatrix} + (i\omega)^{-1}\begin{bmatrix} k & -k \\ -k & k \end{bmatrix}\right]\begin{Bmatrix} V_1 \\ V_2 \end{Bmatrix} = \begin{Bmatrix} F_1 \\ -F_2 \end{Bmatrix} \tag{14}$$

For a system with two masses connected by a spring and damper:

$$\left[i\omega\begin{bmatrix} m & 0 \\ 0 & m \end{bmatrix} + \begin{bmatrix} \eta & -\eta \\ -\eta & \eta \end{bmatrix} + (i\omega)^{-1}\begin{bmatrix} k & -k \\ -k & k \end{bmatrix}\right]\begin{Bmatrix} V_1 \\ V_2 \end{Bmatrix} = \begin{Bmatrix} F_1 \\ -F_2 \end{Bmatrix} \tag{15}$$

Knowing the dynamic stiffness representation then the four-pole parameter representation can be calculated. Thus for the two mass case from above:

$$\begin{Bmatrix} F_1 \\ V_1 \end{Bmatrix} = \begin{bmatrix} 1-\omega^2 m(i\omega\eta + k)^{-1} & -i\omega^3 m^2 (i\omega\eta + k)^{-1} \\ i\omega(k + i\omega\eta)^{-1} & 1-\omega^2 m(i\omega\eta + k)^{-1} \end{bmatrix}\begin{Bmatrix} F_2 \\ V_2 \end{Bmatrix} \tag{16}$$

In the next section this same approach will be taken to determine the general transmissibility matrix for a viscoelastic isolator constrained between two rigid surfaces.

5.3.3 Theoretical Development of the General Transmissibility Matrix

In this section the general 24x24 transmissibility matrix for a viscoelastic isolator will be derived from the equation of motion expressed in the frequency domain. The vibration isolator system will be assumed to comprise the isolator itself and the the two surfaces against which the isolator acts. It will be assumed that these surfaces may be considered to be rigid with respect to the behaviour of the isolator.

The following equation, which describes the deformation of the isolation system, can be developed in frequency domain. Initially it will be assumed that the surfaces above and below the isolators are elastic.

$$[-\omega^2\mathbf{M} + \mathbf{K}_e + \sum_{j=1}^{N_t}\mathbf{K}_{vj}G_j^*(t)]\ddot{\mathbf{A}} = \mathbf{F} \tag{17}$$

Where:

$$\mathbf{M} = \begin{bmatrix} \mathbf{M}_{tt} & \mathbf{M}_{tc} & \mathbf{0} & \mathbf{0} & \mathbf{0} \\ \mathbf{M}_{ct} & \mathbf{M}_{cc}^t + \mathbf{M}_{vv}^t & \mathbf{M}_{cv}^t & \mathbf{0} & \mathbf{0} \\ \mathbf{0} & \mathbf{M}_{vc}^t & \mathbf{M}_{vv} & \mathbf{M}_{vc}^b & \mathbf{0} \\ \mathbf{0} & \mathbf{0} & \mathbf{M}_{vc}^b & \mathbf{M}_{cc}^b + \mathbf{M}_{vv}^b & \mathbf{M}_{cb} \\ \mathbf{0} & \mathbf{0} & \mathbf{0} & \mathbf{M}_{bc} & \mathbf{M}_{bb} \end{bmatrix} \qquad \mathbf{K}_e = \begin{bmatrix} \mathbf{K}_{tt} & \mathbf{K}_{tc} & \mathbf{0} & \mathbf{0} & \mathbf{0} \\ \mathbf{K}_{ct} & \mathbf{K}_{cc}^t & \mathbf{0} & \mathbf{0} & \mathbf{0} \\ \mathbf{0} & \mathbf{0} & \mathbf{0} & \mathbf{0} & \mathbf{0} \\ \mathbf{0} & \mathbf{0} & \mathbf{0} & \mathbf{K}_{cc}^b & \mathbf{K}_{cb} \\ \mathbf{0} & \mathbf{0} & \mathbf{0} & \mathbf{K}_{bc} & \mathbf{K}_{bb} \end{bmatrix}$$

$$\mathbf{K}_{vj} = \begin{bmatrix} 0 & 0 & 0 & 0 & 0 \\ 0 & K^{t}_{vv} & K^{t}_{cv} & 0 & 0 \\ 0 & K^{t}_{vc} & K_{vv} & K^{b}_{vc} & 0 \\ 0 & 0 & K^{b}_{cv} & K^{b}_{vv} & 0 \\ 0 & 0 & 0 & 0 & 0 \end{bmatrix}_j \qquad \ddot{\mathbf{A}} = \begin{bmatrix} \ddot{\mathbf{A}}_t^T & \ddot{\mathbf{A}}_{tc}^T & \ddot{\mathbf{A}}_v^T & \ddot{\mathbf{A}}_{bc}^T & \ddot{\mathbf{A}}_b^T \end{bmatrix}$$

$$\mathbf{F} = \begin{bmatrix} \mathbf{F}_t^T & \mathbf{0} & \mathbf{0} & \mathbf{0} & \mathbf{F}_b^T \end{bmatrix}$$

where N_g is the number of independent kernels used in the description of the viscoelastic characteristics of the isolator. The subscripts or superscripts t, b, v and c denote the mass of the plate attached to the top of the isolator, the plate attached to the base of the isolator, the isolator which is modeled as a viscoelastic material and the connection boundary respectively. $\ddot{\mathbf{A}}_t$, $\ddot{\mathbf{A}}_b$, $\ddot{\mathbf{A}}_v$, $\ddot{\mathbf{A}}_{tc}$ and $\ddot{\mathbf{A}}_{bc}$ are vectors representing the displacements of the top mass, base mass, isolator, connection points between top mass and isolator, and connection points between base mass and isolator respectively. The isolator is modeled with finite elements in which each finite element node has three translational degrees of freedom. A bold letter is used to denote a matrix or a vector.

From this point on it is assumed that the top and bottom masses behave as rigid bodies and that there is no slip at the isolator boundaries. The displacement of every node located on the top and bottom boundaries can then be represented by a transformation matrix with respect to its centre top and centre base node:

$$\ddot{\mathbf{A}}_{tj} = \mathbf{T}_t \mathbf{U}_t \qquad \ddot{\mathbf{A}}_{bj} = \mathbf{T}_b \mathbf{U}_b \tag{18}$$

where the matrix $\mathbf{T}_t$ is a transformation matrix that describes a rigid connection between the j node and the center node of top, and $\mathbf{T}_b$ is a similar matrix for the base.

Thus Equation (17) becomes

$$-\omega^2 \begin{bmatrix} \mathbf{M}_{tt} & \mathbf{M}_{tv} & \mathbf{0} \\ \mathbf{M}_{vt} & \mathbf{M}_{vv} & \mathbf{M}_{vb} \\ \mathbf{0} & \mathbf{M}_{bv} & \mathbf{M}_{bb} \end{bmatrix} \begin{Bmatrix} \mathbf{U}_t \\ \ddot{\mathbf{A}}_v \\ \mathbf{U}_b \end{Bmatrix} + \sum_{j=1}^{N_g} \begin{bmatrix} \mathbf{K}_{tt} & \mathbf{K}_{tv} & \mathbf{0} \\ \mathbf{K}_{vt} & \mathbf{K}_{vv} & \mathbf{K}_{vb} \\ \mathbf{0} & \mathbf{K}_{bv} & \mathbf{K}_{bb} \end{bmatrix}_j G^*_j(i\omega) \begin{Bmatrix} \mathbf{U}_t \\ \ddot{\mathbf{A}}_v \\ \mathbf{U}_b \end{Bmatrix} = \begin{Bmatrix} \mathbf{F}_t \\ \mathbf{0} \\ \mathbf{F}_b \end{Bmatrix} \tag{19}$$

From the second line of the above equation, we get

$$\ddot{\mathbf{A}}_v = \mathbf{T}_t(i\omega)\mathbf{U}_t + \mathbf{T}_b(i\omega)\mathbf{U}_b \tag{20}$$

$$\mathbf{T}_t(i\omega) = -[-\omega^{-2}\mathbf{M}_{vv} + \sum_{j=1}^{N_g} \mathbf{K}_{vvj} G^*_j(i\omega)]^{-1}[-\omega^{-2}\mathbf{M}_{vt} + \sum_{j=1}^{N_g} \mathbf{K}_{vtj} G^*_j(i\omega)] \tag{21}$$

$$\mathbf{T}_b(i\omega) = -[-\omega^{-2}\mathbf{M}_{vv} + \sum_{j=1}^{N_g} \mathbf{K}_{vvj} G^*_j(i\omega)]^{-1}[-\omega^{-2}\mathbf{M}_{vb} + \sum_{j} \mathbf{K}_{vbj} G^*_j(i\omega)] \tag{22}$$

Then we have

$$\mathbf{b}_{11} = \{-\omega^{-2}\mathbf{M}_{tt} + \sum_{j=1}^{N_g} \mathbf{K}_{ttj} G^*_j(i\omega) + [-\omega^{-2}\mathbf{M}_{tv} + \sum_{j=1}^{N_g} \mathbf{K}_{tvj} G^*_j(i\omega)]\mathbf{T}_t(i\omega)\} / i\omega$$

P516303.PDF [Page: 31 of 70]

$$\mathbf{b}_{12} = [-\omega^{-2}\mathbf{M}_{tv} + \sum_{j=1}^{N_s} \mathbf{K}_{tvj} G_j^*(i\omega)]\mathbf{T}_b(i\omega)/i\omega$$

$$\mathbf{b}_{21} = [-\omega^{-2}\mathbf{M}_{bv} + \sum_{j=1}^{N_s} \mathbf{K}_{bvj} G_j^*(i\omega)]\mathbf{T}_t(i\omega)/i\omega = \mathbf{b}_{12}{}^T$$

$$\mathbf{b}_{22} = \{-\omega^{-2}\mathbf{M}_{bb} + \sum_{j=1}^{N_s} \mathbf{K}_{bbj} G_j^*(i\omega) + [-\omega^{-2}\mathbf{M}_{bv} + \sum_{j=1}^{N_s} \mathbf{K}_{bvj} G_j^*(i\omega)]\mathbf{T}_b(i\omega)\}/i\omega$$

Equation (19) may then be written:

$$\begin{bmatrix} \mathbf{b}_{11} & \mathbf{b}_{12} \\ \mathbf{b}_{21} & \mathbf{b}_{22} \end{bmatrix} \begin{Bmatrix} \mathbf{V}_t \\ \mathbf{V}_b \end{Bmatrix} = \begin{Bmatrix} \mathbf{F}_t \\ \mathbf{F}_b \end{Bmatrix} \tag{23}$$

in which $\mathbf{V}_l = i\omega\mathbf{U}_l \quad l = \mathbf{t}, \mathbf{b}$.

As described in section 5.3.2, the transmissibility parameter matrix can be derived from this equation by letting $\mathbf{V}_1 = \mathbf{V}_t$, $\mathbf{V}_2 = \mathbf{V}_b$, $\mathbf{F}_1 = \mathbf{F}_t$ and $\mathbf{F}_2 = -\mathbf{F}_b$.

5.3.4 General Transmissibility Based upon Measured Four Pole Parameter Data

When using experimental procedures to measure the transmissibility matrix, it is difficult to determine the complete matrix as described in Equation (2). For present purposes it will be assumed that three independent cases can be measured. For the j th individual isolator, it is assumed that its four-pole parameter matrix in the x, y and z directions can be measured experimentally. In these tests the base of the isolator is fixed and forces are applied to the top of the isolator in the x, y, and z directions in such a manner that rotations are restrained during deformation due to the forces. Thus the following matrices are available:

$$\begin{Bmatrix} F_{xin} \\ V_{xin} \end{Bmatrix}_j = \begin{bmatrix} a_{x11} & a_{x12} \\ a_{x21} & a_{x22} \end{bmatrix}_j \begin{Bmatrix} F_{xout} \\ V_{xout} \end{Bmatrix}_j \tag{24}$$

$$\begin{Bmatrix} F_{yin} \\ V_{yin} \end{Bmatrix}_j = \begin{bmatrix} a_{y11} & a_{y12} \\ a_{y21} & a_{y22} \end{bmatrix}_j \begin{Bmatrix} F_{yout} \\ V_{yout} \end{Bmatrix}_j \tag{25}$$

$$\begin{Bmatrix} F_{zin} \\ V_{zin} \end{Bmatrix}_j = \begin{bmatrix} a_{z11} & a_{z12} \\ a_{z21} & a_{z22} \end{bmatrix}_j \begin{Bmatrix} F_{zout} \\ V_{zout} \end{Bmatrix}_j \tag{26}$$

Of interest is how well this data can represent the overall behavior of the engine-raft system.

Each of the above equations can be rewritten as:

$$\begin{bmatrix} b_{l11} & b_{l12} \\ b_{l21} & b_{l22} \end{bmatrix}_j \begin{Bmatrix} V_{lin} \\ V_{lout} \end{Bmatrix}_j = \begin{Bmatrix} F_{lin} \\ -F_{lout} \end{Bmatrix}_j \qquad l = x, y, z \tag{27}$$

where:

$$\begin{bmatrix} b_{l11} & b_{l12} \\ b_{l21} & b_{l22} \end{bmatrix}_j = \begin{bmatrix} a_{l11}a_{l21}^{-1} & a_{l12} - a_{l11}a_{l21}^{-1}a_{l22} \\ -a_{l21}^{-1} & a_{l21}^{-1}a_{l22} \end{bmatrix}_j \qquad l = x, y, z \tag{28}$$

hence:

$$\begin{bmatrix} \hat{\mathbf{b}}_{11} & \mathbf{0} & \hat{\mathbf{b}}_{12} & \mathbf{0} \\ \mathbf{0} & \mathbf{0} & \mathbf{0} & \mathbf{0} \\ \hat{\mathbf{b}}_{21} & \mathbf{0} & \hat{\mathbf{b}}_{22} & \mathbf{0} \\ \mathbf{0} & \mathbf{0} & \mathbf{0} & \mathbf{0} \end{bmatrix}_j \begin{Bmatrix} \mathbf{V}_{in} \\ \mathbf{V}_{out} \end{Bmatrix}_j = \begin{Bmatrix} \mathbf{F}_{in} \\ -\mathbf{F}_{out} \end{Bmatrix}_j \tag{29}$$

where:

$$\hat{\mathbf{b}}_{lmj} = \begin{bmatrix} b_{xlm} & 0 & 0 \\ 0 & b_{ylm} & 0 \\ 0 & 0 & b_{zlm} \end{bmatrix}_j \qquad l = 1,2;\ m = 1,2 \tag{30}$$

and those components related to moments in $\mathbf{F}_{inj}$ and $\mathbf{F}_{outj}$ are zero.

5.3.5 Parallel Assemblies of Isolators

In the engine-isolator-raft system, each layer of isolators is considered as being rigidly connected with the engine, raft or base. Such a layer of isolators can be considered to act in parallel as shown in Figure 2.

P516303.PDF [Page: 33 of 70]

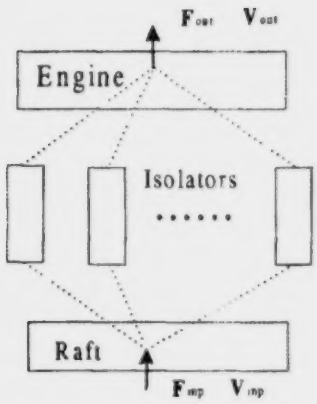

Figure 2 A Layer of Isolators in Parallel between the Engine and the Raft

For an individual isolator, its transmissibility parameter matrix can be written as:

$$\begin{Bmatrix} \mathbf{F}_{in} \\ \mathbf{V}_{in} \end{Bmatrix}_j = \begin{bmatrix} \mathbf{a}_{11} & \mathbf{a}_{12} \\ \mathbf{a}_{21} & \mathbf{a}_{22} \end{bmatrix}_j \begin{Bmatrix} \mathbf{F}_{out} \\ \mathbf{V}_{out} \end{Bmatrix}_j \tag{31}$$

which can be rewritten as:

$$\begin{bmatrix} \mathbf{b}_{11} & \mathbf{b}_{12} \\ \mathbf{b}_{21} & \mathbf{b}_{22} \end{bmatrix}_j \begin{Bmatrix} \mathbf{V}_{in} \\ \mathbf{V}_{out} \end{Bmatrix}_j = \begin{Bmatrix} \mathbf{F}_{in} \\ -\mathbf{F}_{out} \end{Bmatrix}_j \tag{32}$$

For the case discussed in Section 5.3.3, Equation (32) corresponds to Equation (23), where:

$$\begin{bmatrix} \mathbf{b}_{11} & \mathbf{b}_{12} \\ \mathbf{b}_{21} & \mathbf{b}_{22} \end{bmatrix}_j = \begin{bmatrix} \mathbf{a}_{11}\mathbf{a}_{21}^{-1} & \mathbf{a}_{12} - \mathbf{a}_{11}\mathbf{a}_{21}^{-1}\mathbf{a}_{22} \\ -\mathbf{a}_{21}^{-1} & \mathbf{a}_{21}^{-1}\mathbf{a}_{22} \end{bmatrix}_j$$

and for the case in Section 5.3.4, it corresponds to Equation (29), where

$$\begin{bmatrix} \mathbf{b}_{11} & \mathbf{b}_{12} \\ \mathbf{b}_{21} & \mathbf{b}_{22} \end{bmatrix}_j = \begin{bmatrix} \hat{\mathbf{b}}_{11} & \mathbf{0} & \hat{\mathbf{b}}_{12} & \mathbf{0} \\ \mathbf{0} & \mathbf{0} & \mathbf{0} & \mathbf{0} \\ \hat{\mathbf{b}}_{21} & \mathbf{0} & \hat{\mathbf{b}}_{22} & \mathbf{0} \\ \mathbf{0} & \mathbf{0} & \mathbf{0} & \mathbf{0} \end{bmatrix}_j$$

Based upon the geometry of the system there exist the following relationships between the forces and the velocities of the individual isolators and the forces and velocities of the engine and the raft:

$$\mathbf{F}_{in} = \sum_{j=1}^{J} \begin{bmatrix} \mathbf{I} & \mathbf{0} \\ \mathbf{T}_{f1} & \mathbf{I} \end{bmatrix}_j \mathbf{F}_{inj} \qquad \mathbf{V}_{inj} = \begin{bmatrix} \mathbf{I} & \mathbf{T}_{v1} \\ \mathbf{0} & \mathbf{I} \end{bmatrix}_j \mathbf{V}_{in} \tag{33}$$

$$\mathbf{F}_{out} = \sum_{j=1}^{J} \begin{bmatrix} \mathbf{I} & \mathbf{0} \\ \mathbf{T}_{f2} & \mathbf{I} \end{bmatrix}_j \mathbf{F}_{outj} \qquad \mathbf{V}_{outj} = \begin{bmatrix} \mathbf{I} & \mathbf{T}_{v2} \\ \mathbf{0} & \mathbf{I} \end{bmatrix}_j \mathbf{V}_{out} \tag{34}$$

where:

$$\mathbf{T}_{f1_j} = \mathbf{T}_{v1_j} = \begin{bmatrix} 0 & z_1 & -y_1 \\ -z_1 & 0 & x_1 \\ y_1 & -x_1 & 0 \end{bmatrix}_j \qquad \mathbf{T}_{f2_j} = \mathbf{T}_{v2_j} = \begin{bmatrix} 0 & z_2 & -y_2 \\ -z_2 & 0 & x_2 \\ y_2 & -x_2 & 0 \end{bmatrix}_j$$

$$\begin{Bmatrix} x_1 \\ y_1 \\ z_1 \end{Bmatrix}_j = \mathbf{r}_1 - \mathbf{r}_{1j} \qquad \begin{Bmatrix} x_2 \\ y_2 \\ z_2 \end{Bmatrix}_j = \mathbf{r}_2 - \mathbf{r}_{2j} \tag{35}$$

$\mathbf{r}_1$ and $\mathbf{r}_2$ are the location vectors of the centre of mass of the engine and the raft , respectively, (or between the raft and the reference point chosen on the base), and $\mathbf{r}_{1_j}$ and $\mathbf{r}_{2_j}$ are the position vectors that define the location of the top and bottom of the one-dimensional isolator used in VVESACTIVE for the jth isolator.
Thus:

$$\begin{Bmatrix} \mathbf{V}_{in} \\ \mathbf{V}_{out} \end{Bmatrix}_j = \begin{bmatrix} \mathbf{I} & \mathbf{T}_{v1} & \mathbf{0} & \mathbf{0} \\ \mathbf{0} & \mathbf{I} & \mathbf{0} & \mathbf{0} \\ \mathbf{0} & \mathbf{0} & \mathbf{I} & \mathbf{T}_{v2} \\ \mathbf{0} & \mathbf{0} & \mathbf{0} & \mathbf{I} \end{bmatrix}_j \begin{Bmatrix} \mathbf{V}_{in} \\ \mathbf{V}_{out} \end{Bmatrix} \tag{36}$$

and

$$\begin{bmatrix} \tilde{\mathbf{b}}_{11} & \tilde{\mathbf{b}}_{12} \\ \tilde{\mathbf{b}}_{21} & \tilde{\mathbf{b}}_{22} \end{bmatrix}_j \begin{Bmatrix} \mathbf{V}_{in} \\ \mathbf{V}_{out} \end{Bmatrix} = \begin{bmatrix} \mathbf{I} & \mathbf{0} & \mathbf{0} & \mathbf{0} \\ \mathbf{T}_{f1} & \mathbf{I} & \mathbf{0} & \mathbf{0} \\ \mathbf{0} & \mathbf{0} & \mathbf{I} & \mathbf{0} \\ \mathbf{0} & \mathbf{0} & \mathbf{T}_{f2} & \mathbf{I} \end{bmatrix}_j \begin{Bmatrix} \mathbf{F}_{in} \\ -\mathbf{F}_{out} \end{Bmatrix}_j \tag{37}$$

where:

P516303.PDF [Page: 35 of 70]

$$\begin{bmatrix} \tilde{\mathbf{b}}_{11} & \tilde{\mathbf{b}}_{12} \\ \tilde{\mathbf{b}}_{21} & \tilde{\mathbf{b}}_{22} \end{bmatrix}_j = \begin{bmatrix} \mathbf{I} & \mathbf{0} & \mathbf{0} & \mathbf{0} \\ \mathbf{T}_{f1} & \mathbf{I} & \mathbf{0} & \mathbf{0} \\ \mathbf{0} & \mathbf{0} & \mathbf{I} & \mathbf{0} \\ \mathbf{0} & \mathbf{0} & \mathbf{T}_{f2} & \mathbf{I} \end{bmatrix}_j \begin{bmatrix} \mathbf{b}_{11} & \mathbf{b}_{12} \\ \mathbf{b}_{21} & \mathbf{b}_{22} \end{bmatrix}_j \begin{bmatrix} \mathbf{I} & \mathbf{T}_{v1} & \mathbf{0} & \mathbf{0} \\ \mathbf{0} & \mathbf{I} & \mathbf{0} & \mathbf{0} \\ \mathbf{0} & \mathbf{0} & \mathbf{I} & \mathbf{T}_{v2} \\ \mathbf{0} & \mathbf{0} & \mathbf{0} & \mathbf{I} \end{bmatrix}_j \tag{38}$$

Thus:

$$\begin{Bmatrix} \mathbf{F}_{in} \\ -\mathbf{F}_{out} \end{Bmatrix} = \sum_{j=1}^{J} \begin{bmatrix} \mathbf{I} & \mathbf{0} & \mathbf{0} & \mathbf{0} \\ \mathbf{T}_{f1} & \mathbf{I} & \mathbf{0} & \mathbf{0} \\ \mathbf{0} & \mathbf{0} & \mathbf{I} & \mathbf{0} \\ \mathbf{0} & \mathbf{0} & \mathbf{T}_{f2} & \mathbf{I} \end{bmatrix}_j \begin{Bmatrix} \mathbf{F}_{in} \\ -\mathbf{F}_{out} \end{Bmatrix}_j = \sum_{j=1}^{J} \begin{bmatrix} \tilde{\mathbf{b}}_{11} & \tilde{\mathbf{b}}_{12} \\ \tilde{\mathbf{b}}_{21} & \tilde{\mathbf{b}}_{22} \end{bmatrix}_j \begin{Bmatrix} \mathbf{V}_{in} \\ \mathbf{V}_{out} \end{Bmatrix} = \begin{bmatrix} \mathbf{B}_{11} & \mathbf{B}_{12} \\ \mathbf{B}_{21} & \mathbf{B}_{22} \end{bmatrix} \begin{Bmatrix} \mathbf{V}_{in} \\ \mathbf{V}_{out} \end{Bmatrix} \tag{39}$$

From which the required transmissibility matrix can be found:

$$\begin{Bmatrix} \mathbf{F}_{in} \\ \mathbf{V}_{in} \end{Bmatrix} = \begin{bmatrix} \mathbf{A}_{11} & \mathbf{A}_{12} \\ \mathbf{A}_{21} & \mathbf{A}_{22} \end{bmatrix} \begin{Bmatrix} \mathbf{F}_{out} \\ \mathbf{V}_{out} \end{Bmatrix} \tag{40}$$

in which:

$$\begin{bmatrix} \mathbf{A}_{11} & \mathbf{A}_{12} \\ \mathbf{A}_{21} & \mathbf{A}_{22} \end{bmatrix} = \begin{bmatrix} -\mathbf{B}_{11}\mathbf{B}_{21}^{-1} & \mathbf{B}_{12} - \mathbf{B}_{11}\mathbf{B}_{21}^{-1}\mathbf{B}_{22} \\ -\mathbf{B}_{21}^{-1} & -\mathbf{B}_{21}^{-1}\mathbf{B}_{22} \end{bmatrix} \tag{41}$$

5.3.6 Equations Governing Transmission Characteristics of Complete System

In the engine-isolator-raft-isolator-ground system, both the engine and the raft are treated as rigid bodies with mass and rotational inertia. For such rigid bodies, there exist the following relationship between input and output:

$$i\omega \mathbf{M}_e \mathbf{V}_e = \mathbf{F}_1 - \mathbf{F}_2$$

where $\mathbf{F}_1$ and $\mathbf{F}_2$ act on the center of gravity of the body, and $\mathbf{V}_e = \mathbf{V}_1 = \mathbf{V}_2$.

Thus, its transmissibility matrix will be:

$$\begin{Bmatrix} \mathbf{F}_1 \\ \mathbf{V}_1 \end{Bmatrix} = \begin{bmatrix} \mathbf{I} & i\omega \mathbf{M}_e \\ \mathbf{0} & \mathbf{I} \end{bmatrix} \begin{Bmatrix} \mathbf{F}_2 \\ \mathbf{V}_2 \end{Bmatrix} \tag{42}$$

If the local coordinates are coincided with the principal axes of inertia of the body, the mass matrix $\mathbf{M}_e$ is diagonal.

In the following development the velocity and force matrices each have six components representing three displacements and three rotations or their equivalent forces. Considering each component in turn:

a) Engine

Input: $\mathbf{F}_4$, $\mathbf{V}_4$ Output: $\mathbf{F}_5$, $\mathbf{V}_5$

$$\begin{Bmatrix}\mathbf{F}_4\\ \mathbf{V}_4\end{Bmatrix}=\begin{bmatrix}\mathbf{I} & i\omega\mathbf{M}_e^{\,e}\\ \mathbf{0} & \mathbf{I}\end{bmatrix}\begin{Bmatrix}\mathbf{F}_5\\ \mathbf{V}_5\end{Bmatrix}=\mathbf{P}_4\begin{Bmatrix}\mathbf{F}_5\\ \mathbf{V}_5\end{Bmatrix} \tag{43}$$

where $\mathbf{M}_e^{\,e}$ is the mass matrix of the engine including rotational inertia terms.

b) Isolator Layer 1

Input: $\mathbf{F}_3$, $\mathbf{V}_3$ Output: $\mathbf{F}_4$, $\mathbf{V}_4$

$$\begin{Bmatrix}\mathbf{F}_3\\ \mathbf{V}_3\end{Bmatrix}=\begin{bmatrix}\mathbf{A}^{(1)}{}_{11} & \mathbf{A}^{(1)}{}_{12}\\ \mathbf{A}^{(1)}{}_{21} & \mathbf{A}^{(1)}{}_{22}\end{bmatrix}\begin{Bmatrix}\mathbf{F}_4\\ \mathbf{V}_4\end{Bmatrix}=\mathbf{P}_3\begin{Bmatrix}\mathbf{F}_4\\ \mathbf{V}_4\end{Bmatrix} \tag{44}$$

where the coefficient matrix represents the contribution of all the isolators at this level.

c) Raft

Input: $\mathbf{F}_2$, $\mathbf{V}_2$ Output: $\mathbf{F}_3$, $\mathbf{V}_3$

$$\begin{Bmatrix}\mathbf{F}_2\\ \mathbf{V}_2\end{Bmatrix}=\begin{bmatrix}\mathbf{I} & i\omega\mathbf{M}_e^{\,r}\\ \mathbf{0} & \mathbf{I}\end{bmatrix}\begin{Bmatrix}\mathbf{F}_3\\ \mathbf{V}_3\end{Bmatrix}=\mathbf{P}_2\begin{Bmatrix}\mathbf{F}_3\\ \mathbf{V}_3\end{Bmatrix} \tag{45}$$

where $\mathbf{M}_e^{\,r}$ is the mass matrix of the raft including rotational inertia terms.

d) Isolator Layer 2

Input: $\mathbf{F}_1$, $\mathbf{V}_1$ Output: $\mathbf{F}_2$, $\mathbf{V}_2$

Where $\mathbf{V}_1$ is with respect to a chosen point on the base.

$$\begin{Bmatrix}\mathbf{F}_1\\ \mathbf{V}_1\end{Bmatrix}=\begin{bmatrix}\mathbf{A}^{(2)}{}_{11} & \mathbf{A}^{(2)}{}_{12}\\ \mathbf{A}^{(2)}{}_{21} & \mathbf{A}^{(2)}{}_{22}\end{bmatrix}\begin{Bmatrix}\mathbf{F}_2\\ \mathbf{V}_2\end{Bmatrix}=\mathbf{P}_1\begin{Bmatrix}\mathbf{F}_2\\ \mathbf{V}_2\end{Bmatrix} \tag{46}$$

The equation defining the complete system response is then given by:

$$\begin{Bmatrix}\mathbf{F}_1\\ \mathbf{V}_1\end{Bmatrix}=\mathbf{P}_1\mathbf{P}_2\mathbf{P}_3\mathbf{P}_4\begin{Bmatrix}\mathbf{F}_5\\ \mathbf{V}_5\end{Bmatrix}=\begin{bmatrix}\mathbf{D}_{11} & \mathbf{D}_{12}\\ \mathbf{D}_{21} & \mathbf{D}_{22}\end{bmatrix}\begin{Bmatrix}\mathbf{F}_5\\ \mathbf{V}_5\end{Bmatrix} \tag{47}$$

Where $\mathbf{F}_1$ represent the total forces applied to the base, and $\mathbf{V}_1$ represents the velocities of some chosen point on the base, and $\mathbf{F}_5$, $\mathbf{V}_5$ represent the forces and velocities of the centre of mass of the engine.

From this equation the force and velocity transmissibility functions can be determined.

For velocity frequency response functions $\mathbf{V}_1 = \mathbf{0}$, then:

$$\mathbf{V}_5 = -\mathbf{D}_{22}^{-1}\mathbf{D}_{21}\mathbf{F}_5 = \mathbf{H}\mathbf{F}_5$$

where $\mathbf{H} = -\mathbf{D}_{22}^{-1}\mathbf{D}_{21}$.

For force transmissibility $\mathbf{V}_1 = \mathbf{0}$, then:

$$\mathbf{V}_5 = -\mathbf{D}_{22}^{-1}\mathbf{D}_{21}\mathbf{F}_5 = \mathbf{H}\mathbf{F}_5$$

where $\mathbf{H} = -\mathbf{D}_{22}^{-1}\mathbf{D}_{21}$

Hence :

$$\mathbf{F}_1 = (\mathbf{D}_{11} - \mathbf{D}_{12}\mathbf{D}_{22}^{-1}\mathbf{D}_{21})\mathbf{F}_5 = \mathbf{T}_f\mathbf{F}_5$$

$$\mathbf{T}_f = \mathbf{D}_{11} - \mathbf{D}_{12}\mathbf{D}_{22}^{-1}\mathbf{D}_{21} \qquad (48)$$

is the required force transmissibility matrix between the six degrees of freedom of the centre of mass of the engine and the six degrees of freedom of the base of the lower isolator.

For velocity transmissibility functions $\mathbf{F}_5 = \mathbf{0}$

Whence: $\mathbf{V}_1 = \mathbf{D}_{22}\mathbf{V}_5$ and $\mathbf{V}_5 = \mathbf{D}_{22}^{-1}\mathbf{V}_1 = \mathbf{T}_v\mathbf{V}_1$, thus the velocity transmissibility function between velocities applied at the base of the lower isolator to the centre of mass of the engine is given by:

$$\mathbf{T}_v = \mathbf{D}_{22}^{-1} \qquad (49)$$

5.3.7 Numerical Results

This is an example to illustrate the application of the transmissibility parameter method to the engine-isolator-raft-isolator-ground system shown in Figure 3.

Figure 4 shows the magnitude of its diagonal force transmissibility functions (the diagonal velocity transmissibility functions are the same). Figure 5 shows the magnitude of its frequency response functions.

Figures 6-11 show the comparisons between the results calculated using the full transmissibility matrix calculated from the equations as presented in section 5.3.3 (this corresponds to case 1 of the users manual) and the results obtained assuming that only the three sets of four pole parameter results are used as presented in section 5.3.4 (this corresponds to case 2 of the users manual). The notation "c" is used for the complete set and "s" is used for the four pole set. The comparisons plotted are the diagonal values of the force transmissibility matrix and it should be remembered that these functions do not generally completely determine the force transmissibility because of the presence of non-zero off diagonal terms in the transmissibility matrix. However the diagonal terms often provide a good indication of the transmissibility.

As would be expected the results show that for the vertical force case both analyses predict the same response. This is because in this problem there is no coupling between the vertical force and other degrees of freedom and the response conditions coincide with the measured conditions. As would be expected, the largest differences occur in the case of rotational motions as the four pole data provides no information as to the rotational characteristics of the system.

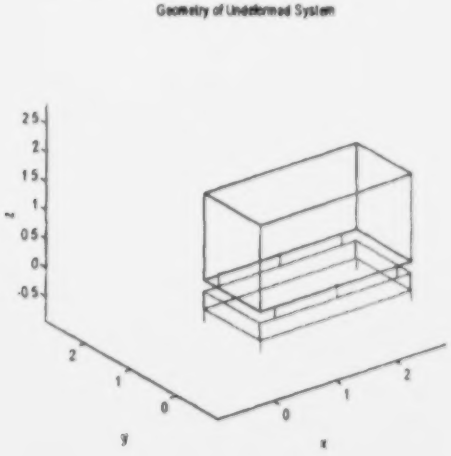

Figure 3 Engine-Isolator-Raft System

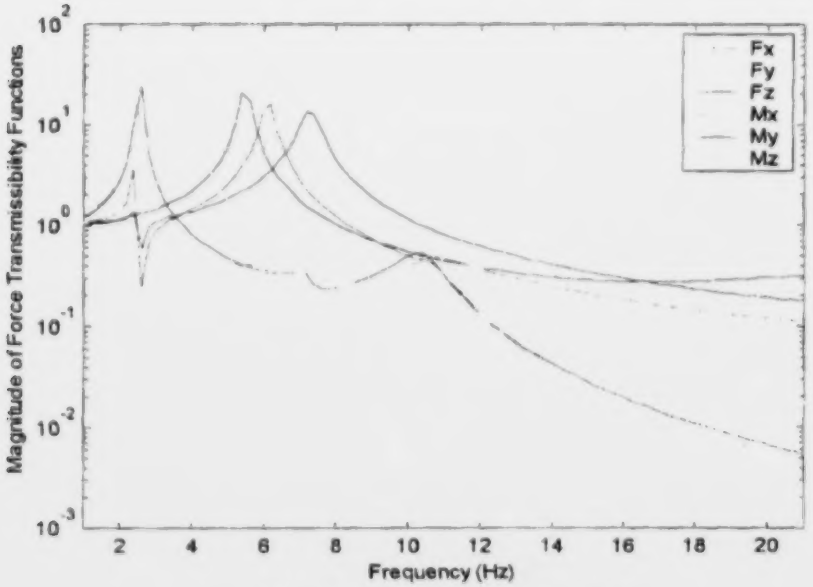

Figure 4 Force Transmissibility Functions

P516303.PDF [Page: 39 of 70]

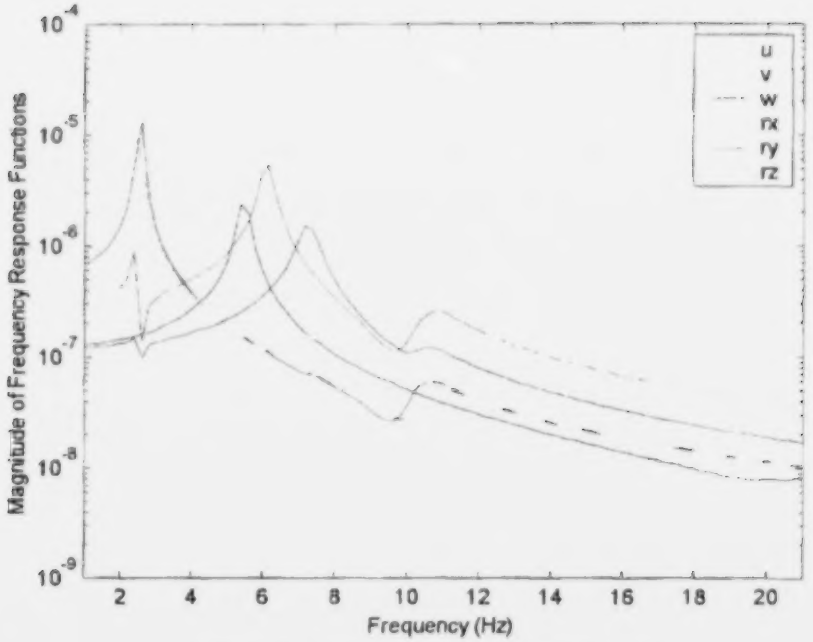

Figure 5 Frequency Response Functions

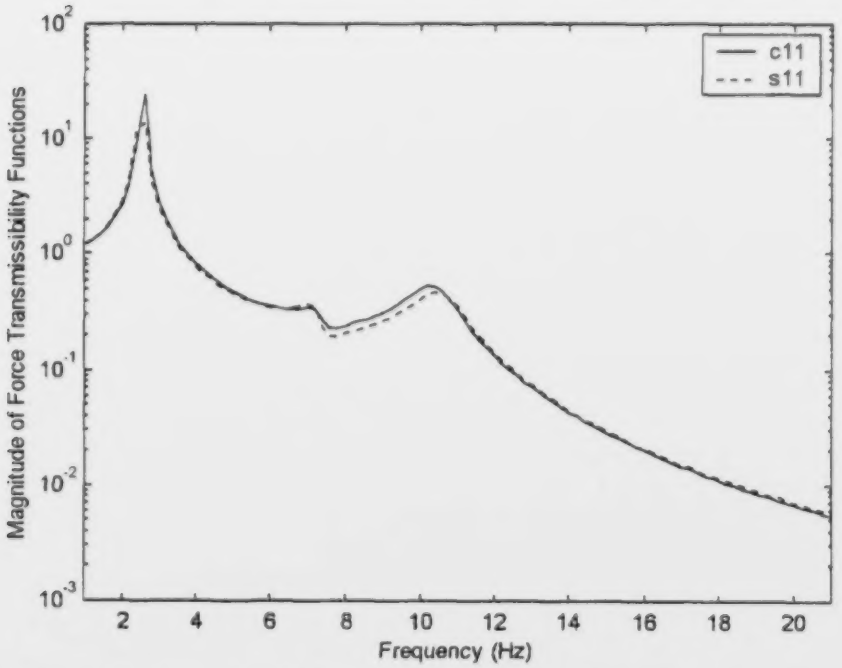

Figure 6 Comparison of Force Transmissibility Function Matrix: x-Force

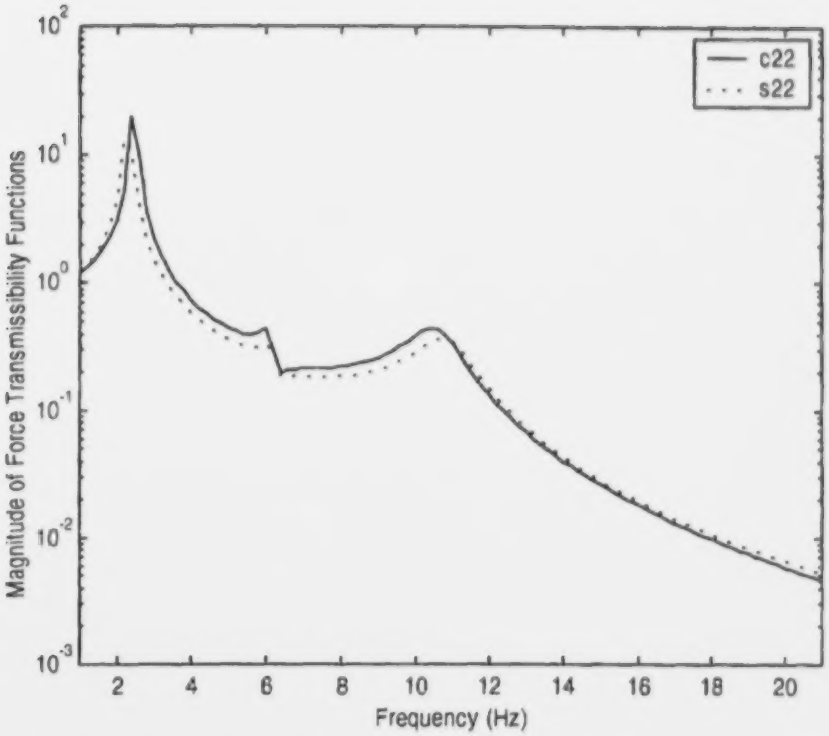

Figure 7 Comparison of Force Transmissibility Function Matrix: y-Force

P516303.PDF [Page: 41 of 70]

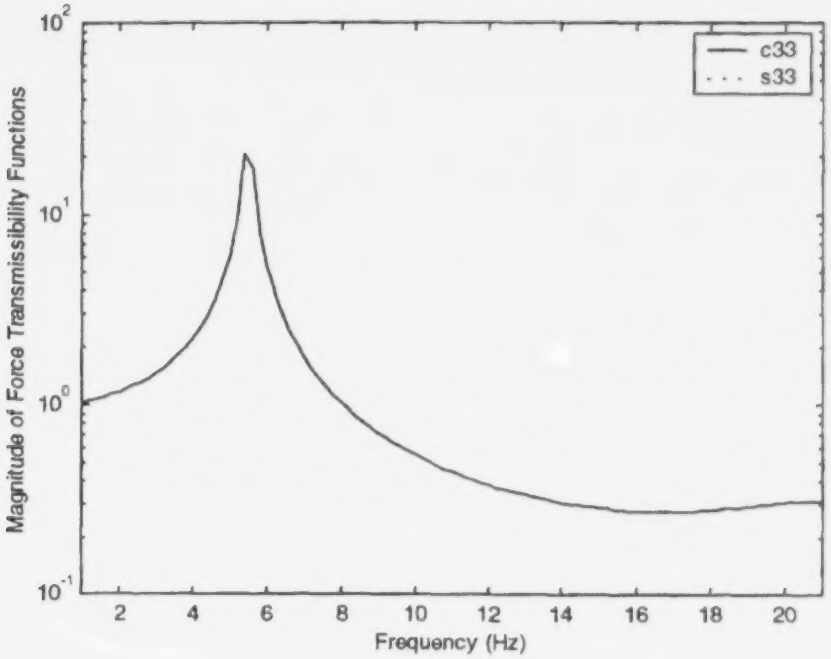

Figure 8 Comparison of Force Transmissibility Function Matrix: z-force

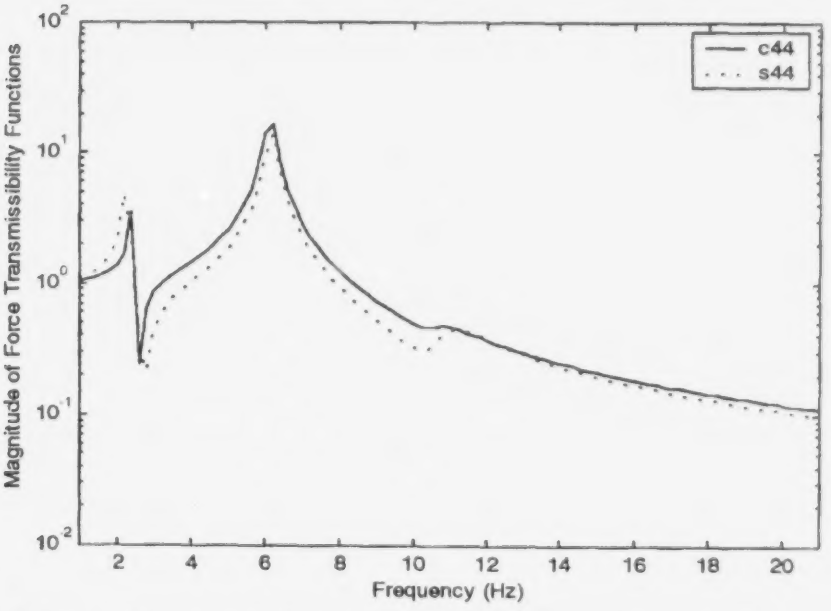

Figure 9 Comparison of Force Transmissibility Function Matrix: x-Moment

P516303.PDF [Page: 42 of 70]

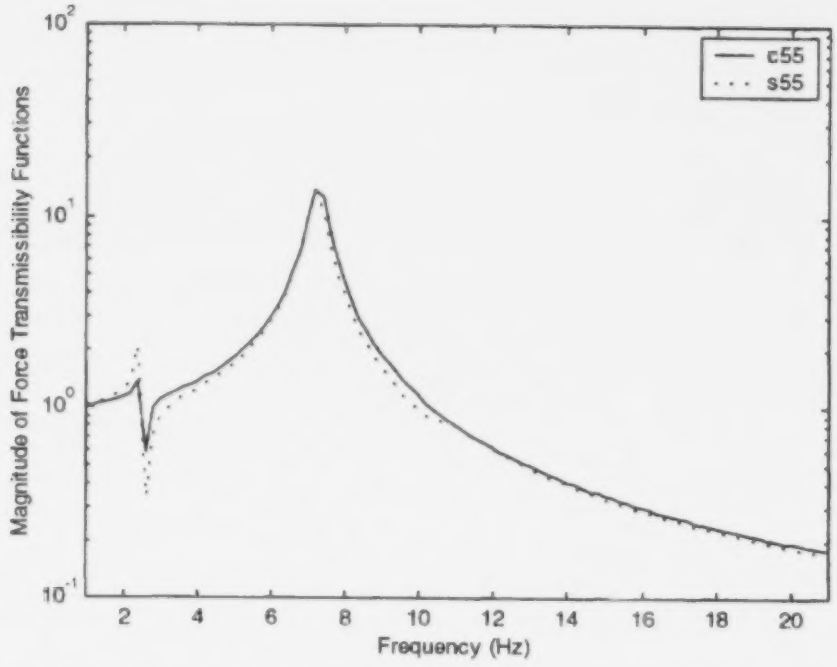

Figure 10 Comparison of Force Transmissibility Function Matrix: y-Moment

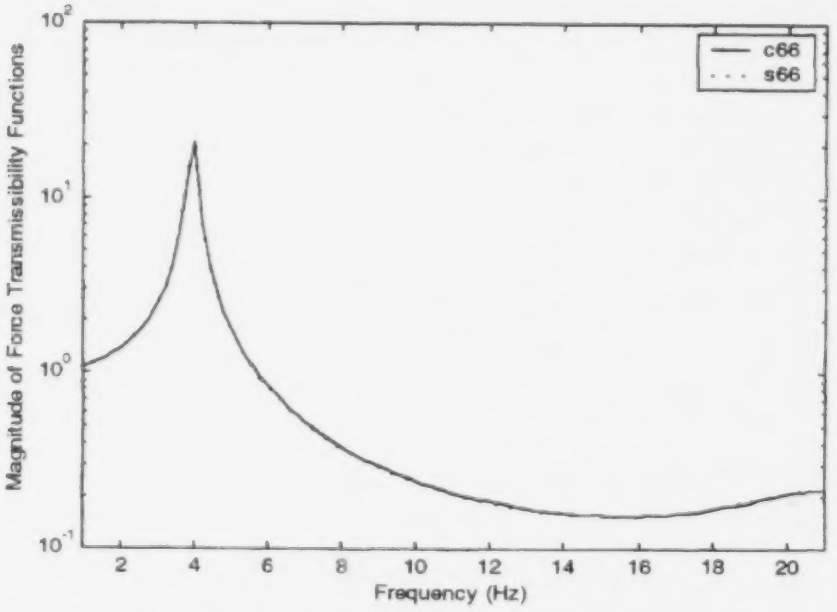

Figure 11 Comparison of Force Transmissibility Function Matrix: z-Moment

P516303.PDF [Page: 43 of 70]

6. Active Control of Transmitted Vibrations

The work on the development of the active control algorithm was conducted by Alain Berry, Professor; Patrice Masson, Assistant Professor; Stéphane Renault, Research Associate from the Department of Mechanical Engineering at the University of Sherbrooke. This section was written by this group.

6.1. Introduction

This chapter documents the theoretical background behind the active control simulation implemented in the VVES software. This software is able to perform feedforward active control simulations in the time domain, in the case of an engine resiliently supported on a raft through vibration isolators. Section 6.2 reviews basic concepts of single-channel feedforward adaptive control. Section 6.3 generalizes the results of single-channel control to multichannel control. Section 6.4 addresses the problem of feedforward adaptive control in the case of a displacement reference sensor on the system.

6.2 Feedforward Adaptive Control

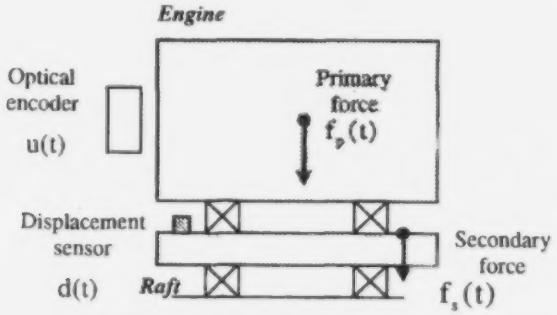

Figure 12 : Model of the system

The system is modeled as shown as figure 12. The *primary force* is denoted $\mathbf{f}_p(t)$ and represents in practice the excitations generated by the motion of some components of the engine (in the general case $\mathbf{f}_p(t)$ has 6 components representing excitation forces and moments in space). The *secondary* (or *control*) *force* is noted $\mathbf{f}_s(t)$; it is the force generated by the control actuator to actively cancel the system dynamics (In the software, $\mathbf{f}_s(t)$ also has 6 components representing control forces and moments in space; the secondary force can be applied at any user-defined position on the engine or on the raft). Also, an option of the software allows for the secondary force to be placed *in parallel* with a given isolator; in this case $\mathbf{f}_s(t)$ is applied simultaneously on the engine and on the raft (in opposite sense), at the location of the isolator. $\mathbf{F}_p(\omega)$ and $\mathbf{F}_s(\omega)$ denote the Fourier transforms of $\mathbf{f}_p(t)$ and $\mathbf{f}_s(t)$.

P515303.PDF [Page: 44 of 70]

In the active control system, the secondary force is driven so as to cancel the displacement $\mathbf{d}(t)$ measured at a chosen point of the system; this sensor is called the *error sensor* and, like the secondary force, it is located at any user-defined position on the engine or on the raft. In feedforward active control systems, the other important component is the *reference sensor* , which provides an advanced information $u(t)$ of the incoming disturbance. For the problem of engine vibration, the reference signal can be measured by an optical encoder placed on the engine, for example. The case of a reference sensor providing a measurement of the engine acceleration at a given point (reference accelerometer) will be considered in a section 6.4. The difference between an optical encoder and an accelerometer on the engine as the reference sensor is that the reference signal is not affected by the control forces in the former case, while it is changed by the control forces in the latter case.

From the principle of linear superposition, the displacement $\mathbf{d}(t)$ is the sum of two displacements $\mathbf{d}_p(t)$ and $\mathbf{d}_s(t)$, where $\mathbf{d}_p(t)$ is the displacement due to the primary force only, and $\mathbf{d}_s(t)$ is the displacement due to the secondary force,

$$\mathbf{d}(t) = \mathbf{d}_p(t) + \mathbf{d}_s(t).$$

In the following, $\mathbf{D}(\omega)$, $\mathbf{D}_p(\omega)$, $\mathbf{D}_s(\omega)$ denote the Fourier transforms of $\mathbf{d}(t)$, $\mathbf{d}_p(t)$ and $\mathbf{d}_s(t)$, respectively. The system can be modeled by two Frequency Response Functions (FRF) $\mathbf{H}(j\omega)$ and $\mathbf{G}(j\omega)$ (Figure 13), where $\mathbf{H}(j\omega)$ is the frequency response function between the primary force and the displacement at the error sensor, and $\mathbf{G}(j\omega)$ is the frequency response function between the secondary force and the displacement at the error sensor. In the case of an actuator placed between the raft and the engine, $\mathbf{G}(j\omega)$ represents the total response at the error sensor due to the force applied on the engine and the force applied on the raft.

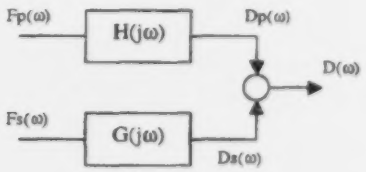

Figure 13: Total displacement response at error sensor as a function of primary and secondary forces

Since the motion of the engine is assumed to be periodic in time, the primary force can be expressed as a combination of harmonics of the engine rotational speed. If only the first three harmonics are considered, it is possible to write :

P516303.PDF [Page 45 of 70]

$$\mathbf{f}_p(t) = \mathbf{A}_1 \cos(\omega_1 t + \varphi_1) + \mathbf{A}_2 \cos(2\omega_1 t + \varphi_2) + \mathbf{A}_3 \cos(3\omega_1 t + \varphi_3) \qquad (50)$$

It is also assumed that the optical encoder provides a reference signal that contains the corresponding harmonics of $\mathbf{f}_p(t)$:

$$u(t) = a_1 \cos(\omega_1 t) + a_2 \cos(2\omega_1 t) + a_3 \cos(3\omega_1 t) \qquad (51)$$

Since $u(t)$ and $\mathbf{f}_p(t)$ have the same frequency content, $\mathbf{f}_p(t)$ can be obtained by passing $u(t)$ through a linear, time-invariant filter **P** which is represented by its frequency response function $\mathbf{P}(j\omega)$. Similarly, the secondary force $\mathbf{f}_s(t)$ is generated by passing the reference $u(t)$ through a filter **W** , see figure 14. The upper branch in Figure 14 represents the physical plant, while the lower branch represents the control path, which has to be implemented in the form of a digital controller.

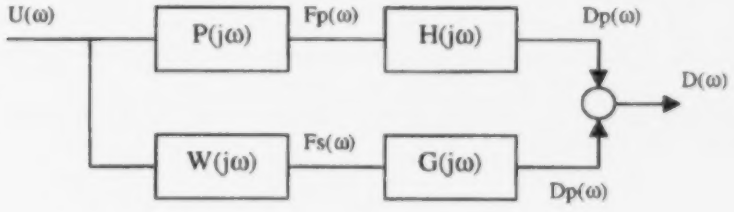

Figure 14 : Total displacement response at error sensor as a function of the reference signal

The problem of deriving an optimal digital controller **W** such that the displacement $\mathbf{d}(t)$ is minimized, is a classical problem in optimal control theory; this problem is discussed in details in [5], therefore only the main results are recalled here. The method usually consists of implementing the controller **W** in the form of a Finite Impulse Response (FIR) filter $\mathbf{W}(z)$, with coefficients that are adapted by a gradient algorithm to minimize a criterion (or cost function):

$$J = E\left[\mathbf{d}(k)^2\right] \qquad (52)$$

where $\mathbf{d}(k)$ is the digitized signal $\mathbf{d}(t)$ and E denotes the mathematical expectation operator. The LMS algorithm therefore consists in updating the filter $\mathbf{W}(z)$ in the direction of the gradient of $J = E\left[\mathbf{d}(k)^2\right]$. It is usual to replace the expectation of $\mathbf{d}(k)^2$ by the instantaneous signal $\mathbf{d}(k)^2$ in order to simplify the update equation. The update equation of the usual LMS algorithm following these assumptions is given by

$$\mathbf{W}(k+1) = \mathbf{W}(k) - \alpha\, \underline{x}(k)\, \mathbf{d}(k), \qquad (53)$$

P516303.PDF [Page: 46 of 70]

where $\underline{x}(k)=[x(k)\ \ x(k-1)\ \ \ldots\ \ x(k-N+1)]^T$, N is the number of filter coefficients in $\mathbf{W}(z)$ and α is a convergence coefficient of the LMS algorithm. The update equation (53) is obtained after permuting the control filter $\mathbf{W}(z)$ and the FRF of the control path $\mathbf{G}(z)$ (Figures 15.a and 15.b), which is possible in the case of time-invariant signals or slowly varying signals. The signal $\underline{x}(k)$ in Equation (53) therefore appears as the reference signal $u(k)$ filtered by the control path $\mathbf{G}(z)$ (Figure 15.b). For this reason, the algorithm is known as the filtered-X LMS (FX-LMS) algorithm.

In practice, the control path $\mathbf{G}(z)$ is also implemented in the form of a Finite Impulse Response (FIR) filter, with coefficients that are derived from a system identification step, realized prior to the control with the primary forces set to zero. In the software, the identification of the control path $\mathbf{G}(z)$ in the form of a FIR filter is done from the FRF $\mathbf{G}(j\omega)$ calculated in VVES.

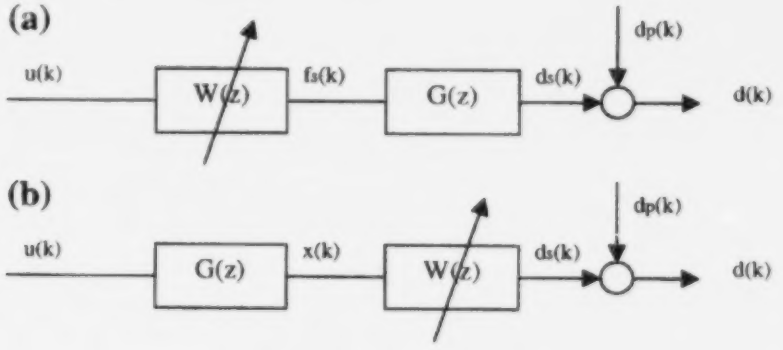

Figure 15 : filtered-X LMS

An important parameter for the time-domain simulation of the FX-LMS algorithm is the adaptation coefficient α in Equation (53), which in practice determines the convergence rate of the active control system: a large coefficient will usually translate into poor control performance, or even divergence of the algorithm, while an excessively small coefficient will translate into a very low convergence rate. The ideal magnitude range of the adaptation coefficient depends on the gain of the control path, therefore it is convenient to introduce a normalized adaptation coefficient λ:

$$\alpha = \frac{\lambda}{\underline{x}^T \underline{x}} \tag{54}$$

The update equation (53) becomes :

$$\mathbf{W}(k+1) = \mathbf{W}(k) - \frac{\lambda}{\underline{x}(k)^T \underline{x}(k)} \underline{x}(k)\, \mathbf{d}(k) \tag{55}$$

This algorithm is known as the normalized FX-LMS algorithm.

P516303.PDF [Page: 47 of 70]

6.3 Multi-Channel Feedforward Adaptive Control

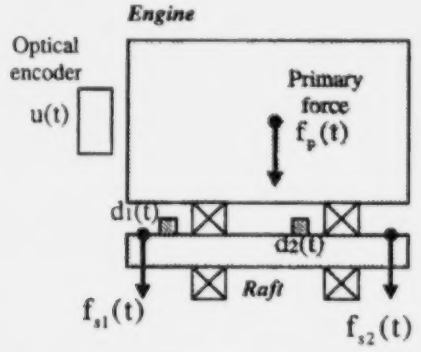

Figure 16 : model of the system with a multichannel control system

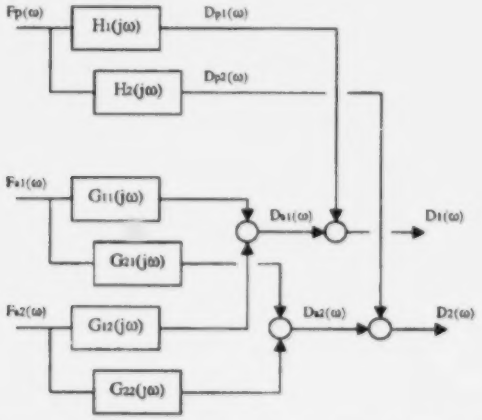

Figure 17: Total displacement response at the error sensors as a function of primary and secondary forces.

If more than one error sensor and control actuator are needed to achieve a better control performance, a multichannel control approach must be used. Figure 16 shows how the system can be modeled in the case of 2 control actuators and 2 error sensors, and figure 17 shows how the total response at the error sensors is related to the primary and control forces. Again, each primary or control force is a generalized excitation consisting of forces or moments applied at user-defined locations. It is possible to generalize this to a problem with N_p primary forces, N_s secondary forces and N_d displacement error sensors using a matrix notation. The matrix representation of figure 17 is shown on figure 18.

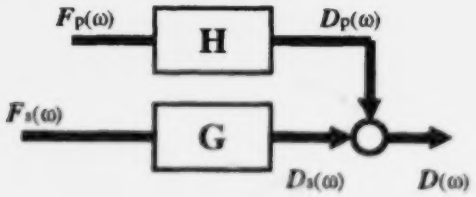

Figure 18 : Matrix representation of the total displacement response at the error sensors as a function of primary and secondary forces for a multichannel system.

In figure 18, the various quantities are defined by :

$$\boldsymbol{F}_P(\omega)=[\mathbf{F}_{P1}(\omega)\quad \mathbf{F}_{P2}(\omega)\quad \ldots\quad \mathbf{F}_{PN_P}(\omega)]^T$$
$$\boldsymbol{F}_S(\omega)=[\mathbf{F}_{S1}(\omega)\quad \mathbf{F}_{S2}(\omega)\quad \ldots\quad \mathbf{F}_{SN_S}(\omega)]^T$$
$$\boldsymbol{D}_P(\omega)=[\mathbf{D}_{P1}(\omega)\quad \mathbf{D}_{P2}(\omega)\quad \ldots\quad \mathbf{D}_{PN_D}(\omega)]^T$$
$$\boldsymbol{D}_S(\omega)=[\mathbf{D}_{S1}(\omega)\quad \mathbf{D}_{S2}(\omega)\quad \ldots\quad \mathbf{D}_{SN_D}(\omega)]^T$$
$$\boldsymbol{D}(\omega)=[\mathbf{D}_1(\omega)\quad \mathbf{D}_2(\omega)\quad \ldots\quad \mathbf{D}_{N_D}(\omega)]^T$$

$$\mathbf{H}=\begin{bmatrix}\mathbf{H}_{11} & \cdots & \mathbf{H}_{1N_P}\\ \cdots & \cdots & \cdots\\ \mathbf{H}_{N_D1} & \cdots & \mathbf{H}_{N_DN_P}\end{bmatrix} \text{ and } \mathbf{G}=\begin{bmatrix}\mathbf{G}_{11} & \cdots & \mathbf{G}_{1N_S}\\ \cdots & \cdots & \cdots\\ \mathbf{G}_{N_D1} & \cdots & \mathbf{G}_{N_DN_S}\end{bmatrix}$$

The matrix **G** represents the control path FRFs between the various secondary actuators and the various error sensors. Like for the single channel case, these individual FRFs are modeled as FIR filters in a preliminary system identification step using the values calculated in VVES. Filtered reference signals x_{ij} are also derived from the reference signal and the control path matrix **G**,

$$\mathbf{x}=\mathbf{G}\mathbf{u}=\begin{bmatrix}\mathbf{x}_{11} & \cdots & \mathbf{x}_{1N_S}\\ \cdots & \cdots & \cdots\\ \mathbf{x}_{N_D1} & \cdots & \mathbf{x}_{N_DN_S}\end{bmatrix}$$ as indicated in figure 19,

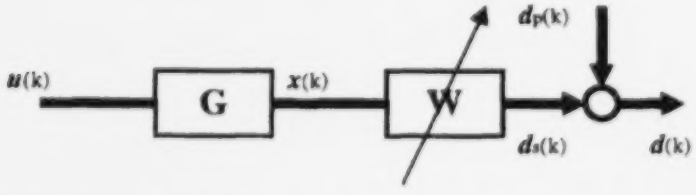

Figure 19 : Feedforward multichannel control system (**W** represents the control filters)

The resulting multichannel adaptive feedforward control system is shown on figure 20,

P516303.PDF [Page: 49 of 70]

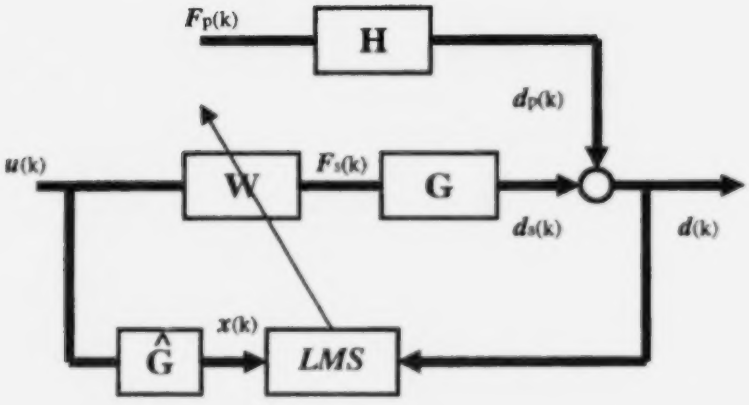

Figure 20 : Multichannel adaptive feedforward control system.

In figure 20, $\hat{\mathbf{G}}$ is an estimate of **G** in the form of a matrix of FIR filters. For the simulation, we take $\hat{\mathbf{G}} = \mathbf{G}$. **W** is a vector of FIR filters :

$$\mathbf{W} = \left[W_1(z)\ \ W_2(z)\ \ \ldots\ \ W_{N_2}(z)\right]^T$$

which coefficients are updated according to the following equation :

$$W_j(k+1) = W_j(k+1) - \lambda \sum_{i=1}^{N_R} \left[\frac{\underline{x}_{ij}(k)}{\underline{x}_{ij}(k)^T\, \underline{x}_{ij}(k)} d_i(k) \right], \qquad (56)$$

with $\underline{x}_{ij}(k) = [x_{ij}(k)\ \ x_{ij}(k-1)\ \ \ldots\ \ x_{ij}(k-N+1)]^T$.

6.4 Multi-Channel Feedforward Adaptive Control with a Displacement Reference Sensor

As stated previously, the case of a reference sensor that measures the displacement response at a given position on the system (instead of an encoder that measures the rotational speed of the engine) is more complex since in this case, the reference signal is affected by the secondary forces. This feedback loop of the control forces on the reference sensor must be compensated in the algorithm. Figure 21 schematically shows the control system in the case of a reference sensor placed on the engine.

P516303.PDF [Page: 50 of 70]

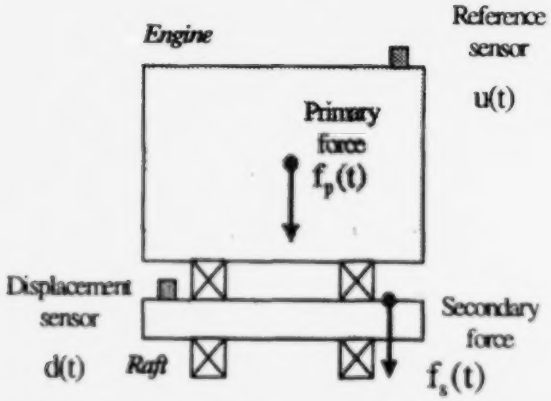

Figure 21 : Model of the system with a displacement reference signal placed on the engine.

Figure 22 shows the multichannel adaptive feedforward control with a displacement reference sensor on the system. In this case, it is necessary to include the FRF between the primary forces and the reference sensor (**R**) and the FRF between the secondary forces and the reference sensor (**S**). Since the reference signal must only reflect the primary forces on the system, it is necessary to subtract an estimate of the effect of secondary forces on the reference sensor from the reference signal $u(k)$. In the simulation, **R** and **S** are implemented in the form of FIR filters, which coefficients are identified from the corresponding FRFs given by VVES.

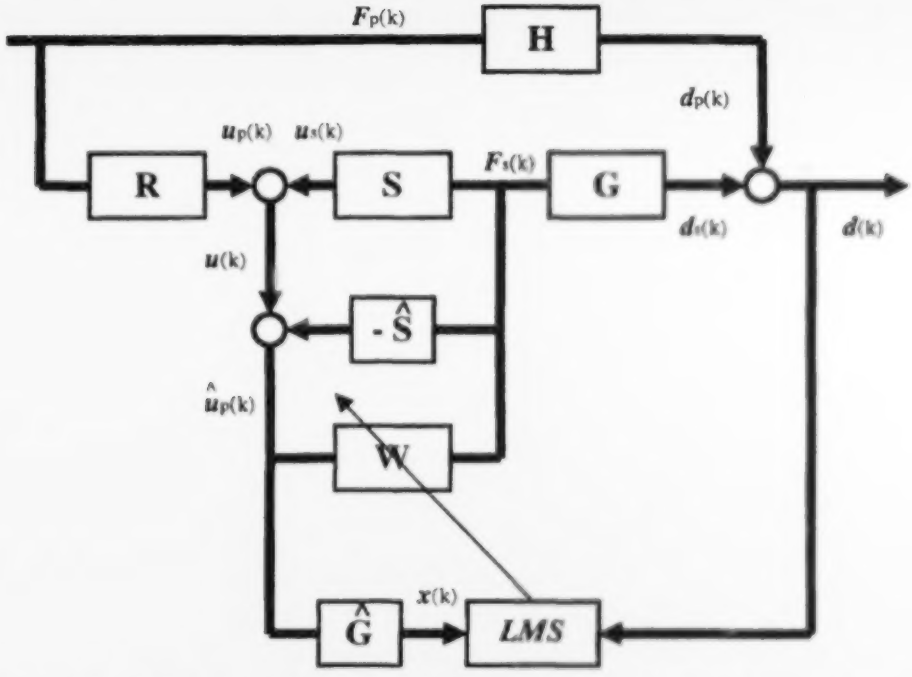

Figure 22 : Multichannel adaptive feedforward control with a displacement reference sensor .

P516303.PDF [Page: 52 of 70]

7. Summary

This report presents a description of a MATLAB based suite of computer programs that are designed to assist in the optimal design of isolators for marine engines. The prime requirement of these programs is to assist in the minimization of the levels of vibration of the engine itself and the levels of vibration that are transmitted from the engine to other parts of the ship. The software developed is designed to provide users with a tool that will enable them to better understand the complicated three dimensional vibration behaviour of the engine and its support system. It also provides quantitative data regarding the levels of transmitted vibration.

The programs developed analyse the behaviour of the combined engine/isolator/raft/isolator/ground system and enables the user to determine:

- the natural frequencies and mode shapes of the complete system
- the frequency response functions between arbitrary points on the engine or on the raft
- the force transmissibility between forces applied to the engine and forces transmitted through individual isolators or the total force transmitted to ground
- the displacement transmissibility between excitation applied at the base and that experienced by the engine
- the ratio of input and output across any individual isolator
- the deflection of the engine due to gravity in times of extreme pitch and roll

With these programs the user will be able to evaluate the effect of different isolator materials and different isolator geometry's and configurations. The capability of the programs to include the behaviour of an independent raft foundation system means that combined complex dynamics of the engine and the raft can be investigated in a convenient manner.

Four specific program groups have been developed in order to provide a range of options with regard to the way in which the characteristics of the isolators are input into the program. These programs are:

- VVESANALYSIS In these programs the properties of the isolators are determined be finite element analysis of the vibration characteristics of the isolators based upon their geometry and based upon constitutive data obtained from the material from which the isolators were fabricated.
- VVESDYNSTFF In these programs the properties of the isolators are based in part upon the measured dynamic stiffness characteristics of the isolator and in part on the basis of analysis.
- VVES4POLE In these programs the properties of the isolators are based in part upon the measured four-pole parameter matrices in given directions and in part on the basis of analysis.
- VVESACTIVE In these programs a feedforward active control program has been developed that enables an assessment to be made of the effect of active control upon the magnitude of the transmitted vibrations.

The range of programs developed represents a sophisticated body of software. It is of value to have such a range of programs in order to make optimal use of the

P516303.PDF [Page: 53 of 70]

results of experimental results where available. Experimental results may, for example, be able to include the effect of such variables as pre-load and temperature variation more accurately than can de done by analysis. On the other hand the experimental data will in general not be sufficient to completely define the isolator characteristics. The approach adopted of combining both sets of results will be most likely to result in reliable data. In those cases where experimental data is not available, for example, in the initial stage of design, a program that is based completely upon fundamental data is required.

In order to verify the accuracy of the output from the programs requires the use of measured data. In this report the numerical consistency of the different programs has been verified by inputting experimental data that was derived from the analytical data. Future work should include comparisons of the results of these programs with experimentally obtained results conducted both upon individual isolators and upon the complete engine – raft system.

7. References

1. Hutton, S.G. "Optimization of Vibration Mount Properties for Application to Shipboard Diesel Engines- Phase II", DREA Contract Report 98/449
2. Bathe, K.J. "Finite Element Procedures", Prentice Hall, Inc. 1996
3. Snowdon, J.C., "Mechanical Four-Pole Parameters and Their Application", Journal of Sound and Vibration, Vol. 15, pp307-323, 1971
4. Dickens, J.D. and Norwood, C.J., "Design of a Test Facility for Vibration Isolator Characterisation", Acoustics Australia. Vol 25(1997), No1, pp23-28
5. Nelson, P.A. and Elliott, S.J. (1992). *Active control of sound.* Academic Press,London.

P516303.PDF [Page: 55 of 70]

APPENDIX 1 Finite Element Modeling of Isolators

General Displacement Finite Element Formulation

The isolators can be modeled in terms of three-dimensional volume elements with displacement functions: $\mathbf{u} = \begin{Bmatrix} u(x,y,z) \\ v(x,y,z) \\ w(x,y,z) \end{Bmatrix}$ (1.1)

For each element, the displacements are represented by

$$\mathbf{u} = \sum_{i=1}^{N} N_i(\xi,\eta,\varsigma) \begin{Bmatrix} u_i \\ v_i \\ w_i \end{Bmatrix} = \sum_{i=1}^{N} N_i(\xi,\eta,\varsigma)\mathbf{u}_i = \mathbf{H}\hat{\mathbf{u}} \tag{1.2}$$

where N is the number of nodes of an element, $\mathbf{u}_i$ is the nodal displacement and $N_i(\xi,\eta,\varsigma)$ is the corresponding shape function. $\mathbf{H}$ is the element shape function matrix, and $\hat{\mathbf{u}}$ is the element nodal displacement vector.

The strains are given by: $\hat{\boldsymbol{\varepsilon}} = \mathbf{D}\mathbf{u}$ (1.3)

where :

$$\mathbf{D} = \begin{bmatrix} \frac{\partial}{\partial x} & 0 & 0 \\ 0 & \frac{\partial}{\partial y} & 0 \\ 0 & 0 & \frac{\partial}{\partial z} \\ \frac{\partial}{\partial y} & \frac{\partial}{\partial x} & 0 \\ 0 & \frac{\partial}{\partial z} & \frac{\partial}{\partial y} \\ \frac{\partial}{\partial z} & 0 & \frac{\partial}{\partial x} \end{bmatrix}$$

Thus

$$\hat{\boldsymbol{\varepsilon}} = \sum_{i=1}^{N} \mathbf{D}N_i(\xi,\eta,\varsigma)\mathbf{u}_i = \sum_{i=1}^{N} \mathbf{B}_i\mathbf{u}_i = \mathbf{B}\hat{\mathbf{u}} \tag{1.4}$$

where $\mathbf{B}$ is the element strain matrix, and

P516303.PDF [Page 56 of 70]

$$\mathbf{B}_i = \begin{bmatrix} N_{i,x} & 0 & 0 \\ 0 & N_{i,y} & 0 \\ 0 & 0 & N_{i,z} \\ N_{i,y} & N_{i,x} & 0 \\ 0 & N_{i,z} & N_{i,y} \\ N_{i,z} & 0 & N_{i,x} \end{bmatrix}$$

The stresses are given by: $\boldsymbol{\sigma} = \mathbf{C}\boldsymbol{\varepsilon} = \sum_{i=1}^{N} \mathbf{C}\mathbf{B}_i\mathbf{u}_i = \sum_{i=1}^{N} \mathbf{S}_i\mathbf{u}_i = \mathbf{S}\hat{\mathbf{u}}$ (1.5)

Where $\mathbf{S}$ is the element stress matrix, and $\mathbf{C}$ is the constitutive matrix. For isotropic materials , there are only two independent constitutive parameters, and:

$$\mathbf{C} = \begin{bmatrix} \lambda+2G & \lambda & \lambda & 0 & 0 & 0 \\ \lambda & \lambda+2G & \lambda & 0 & 0 & 0 \\ \lambda & \lambda & \lambda+2G & 0 & 0 & 0 \\ 0 & 0 & 0 & G & 0 & 0 \\ 0 & 0 & 0 & 0 & G & 0 \\ 0 & 0 & 0 & 0 & 0 & G \end{bmatrix} \quad (1.6)$$

$$\lambda = \frac{E\nu}{(1+\nu)(1-2\nu)} \qquad G = \frac{E}{2(1+\nu)}$$

where E, G, and ν are Young's modulus, the shear modulus and Poisson's ratio, respectively.

The element stiffness matrix can then be shown to be:

$$\mathbf{K}_e = \int_V \mathbf{B}^T\mathbf{S}dV = \int_V \mathbf{B}^T\mathbf{C}\mathbf{B}dV \quad (1.7)$$

When ν tends to 0.5, λ tends to infinity corresponding to the case where the material is incompressible. In practice as Poisson's Ratio approaches .5 numerical problems will arise in the calculations. This problem is usually referred to as a "locking" phenomenon. To solve this problem, a mixed finite element method is required in which both the displacement and the pressure are independently modeled.

Finite Element Formulation for Almost Incompressible Materials

If the body is made of an almost incompressible material, the volumetric strain ε_v and the deviatoric strains $\boldsymbol{\varepsilon}'$ are used to describe its deformations:

$$\varepsilon_v = \varepsilon_{xx} + \varepsilon_{yy} + \varepsilon_{zz} \quad (1.8)$$

P516301.PDF [Page: 57 of 70]

$$\varepsilon'_{ij} = \varepsilon_{ij} - \frac{\varepsilon_v}{3}\delta_{ij} \tag{1.9}$$

where δ_{ij} is the Kronecker delta.

The pressure in the body is defined as:

$$p = -\frac{1}{3}(\sigma_{xx} + \sigma_{yy} + \sigma_{zz}) = -\kappa\varepsilon_v \tag{1.10}$$

where κ is the bulk modulus

$$\kappa = \frac{E}{3(1-2\nu)}$$

and the relationship between deviatoric stresses and deviatoric strains is

$$\mathbf{\acute{o}} = \mathbf{C}'\mathbf{\acute{a}} \tag{1.11}$$

$$\mathbf{C}' = \begin{bmatrix} 2G & 0 & 0 & 0 & 0 & 0 \\ 0 & 2G & 0 & 0 & 0 & 0 \\ 0 & 0 & 2G & 0 & 0 & 0 \\ 0 & 0 & 0 & G & 0 & 0 \\ 0 & 0 & 0 & 0 & G & 0 \\ 0 & 0 & 0 & 0 & 0 & G \end{bmatrix} \tag{1.12}$$

The displacement interpolation is unchanged from the pure displacement formulation:

$$\mathbf{u} = \mathbf{H}\hat{\mathbf{u}} = \sum_{i=1}^{N} N_i(\xi,\eta,\zeta)\mathbf{u}_i \tag{1.13}$$

We can calculate

$$\mathbf{\acute{a}}' = \mathbf{B}_D\hat{\mathbf{u}} = \sum_{i=1}^{N} \mathbf{B}_{Di}\mathbf{u}_i \tag{1.14}$$

in which

$$\mathbf{B}_{Di} = \begin{bmatrix} \frac{2}{3}N_{i,x} & -\frac{1}{3}N_{i,y} & -\frac{1}{3}N_{i,z} \\ -\frac{1}{3}N_{i,x} & \frac{2}{3}N_{i,y} & -\frac{1}{3}N_{i,z} \\ -\frac{1}{3}N_{i,x} & -\frac{1}{3}N_{i,y} & \frac{2}{3}N_{i,z} \\ N_{i,y} & N_{i,x} & 0 \\ 0 & N_{i,z} & N_{i,y} \\ N_{i,z} & 0 & N_{i,x} \end{bmatrix}$$

and

$$\varepsilon_v = \mathbf{B}_V\hat{\mathbf{u}} = \sum_{i=1}^{N} \mathbf{B}_{Vi}\mathbf{u}_i \tag{1.15}$$

in which

$$\mathbf{B}_{Vi} = \begin{bmatrix} N_{i,x} & N_{i,y} & N_{i,z} \end{bmatrix}$$

The pressure interpolation:

P516303.PDF [Page: 58 of 70]

$$p = \mathbf{H}_p \hat{\mathbf{p}} = \sum_{i=1}^{N} H_i(x, y, z) p_i \tag{1.16}$$

The Hu-Washizu variational principle is used to generate the required stiffness equations for the mixed displacement/pressure interpolation finite element:

$$\Pi^*(u, p) = \tfrac{1}{2} \int \hat{\mathbf{a}}'^T \mathbf{C}' \hat{\mathbf{a}}' dV - \tfrac{1}{2} \int p^2 \kappa \, dV - \int p \varepsilon_v dV - \int \mathbf{u}^T \mathbf{f}_B dV - \int \mathbf{u}_s^T \mathbf{f}_s dS \tag{1.17}$$

The resulting "stiffness"equation is:

$$\begin{bmatrix} \mathbf{K}_{uu} & \mathbf{K}_{up} \\ \mathbf{K}_{pu} & \mathbf{K}_{pp} \end{bmatrix} \begin{Bmatrix} \hat{\mathbf{u}} \\ \hat{\mathbf{p}} \end{Bmatrix} = \begin{Bmatrix} \mathbf{F} \\ \mathbf{0} \end{Bmatrix} \tag{1.18}$$

where

$$\begin{aligned} \mathbf{K}_{uu} &= \int_V \mathbf{B}_D^T \mathbf{C}' \mathbf{B}_D dV \\ \mathbf{K}_{up} &= \mathbf{K}_{pu}^T = -\int_V \mathbf{B}_V^T \mathbf{H}_p dV \\ \mathbf{K}_{pp} &= -\int_V \mathbf{H}_p^T \kappa^{-1} \mathbf{H}_p dV \end{aligned} \tag{1.19}$$

Thus, the element stiffness matrix will be

$$\mathbf{K}_e = \mathbf{K}_{uu} - \mathbf{K}_{up} \mathbf{K}_{pp}^{-1} \mathbf{K}_{pu} \tag{1.20}$$

Elements Types

Two kinds of brick finite element are used: a 20-node parabolic solid and 15-node parabolic wedge. According to Bathe [2] only a constant pressure interpolation within the element will give satisfactory answers with these elements. Numerical experimentation with linear and parabolic pressure distributions confirmed this to be the case.

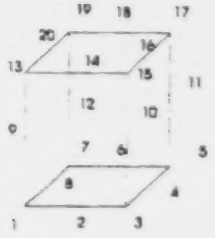

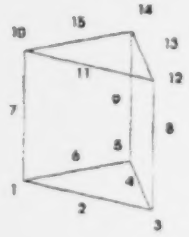

20-node Quadratic Right Prism Element

Shape functions:

$$N_i = \tfrac{1}{8}(1 + \xi_0 \xi)(1 + \eta_0 \eta)(1 + \zeta_0 \zeta)(\xi_0 + \eta_0 + \zeta_0 - 2) \qquad i = 1, 3, 5, 7, 13, 15, 17, 19$$

P516303.PDF [Page: 59 of 70]

$$N_i = \tfrac{1}{4}(1-\xi^2)(1+\eta_0)(1+\zeta_0) \quad i=2,4,14,18$$
$$N_i = \tfrac{1}{4}(1+\xi_0)(1-\eta^2)(1+\zeta_0) \quad i=4,8,16,20$$
$$N_i = \tfrac{1}{4}(1+\xi_0)(1+\eta_0)(1-\zeta^2) \quad i=9,10,11,12 \qquad (1.21)$$

where

$$\xi_0 = \xi_i\xi \qquad \eta_0 = \eta_i\eta \qquad \zeta_0 = \zeta_i\zeta$$

and for each node, the value of (ξ, η, ζ) is listed as follows:

Node	ξ	η	ζ
1	-1	-1	-1
2	0	-1	-1
3	1	-1	-1
4	1	0	-1
5	1	1	-1
6	0	1	-1
7	-1	1	-1
8	-1	0	-1
9	-1	-1	0
10	1	-1	0
11	1	1	0
12	-1	1	0
13	-1	-1	1
14	0	-1	1
15	1	-1	1
16	1	0	1
17	1	1	1
18	0	1	1
19	-1	1	1
20	-1	0	1

15-node Quadratic Triangular Prism Element

Shape functions:

$$N_i = \tfrac{1}{2}L_1(2L_1-)(1+\zeta_0) - \tfrac{1}{2}L_1(1-\zeta^2) \quad i=1,10$$
$$N_i = \tfrac{1}{2}L_2(2L_2-)(1+\zeta_0) - \tfrac{1}{2}L_2(1-\zeta^2) \quad i=3,12$$
$$N_i = \tfrac{1}{2}L_3(2L_3-)(1+\zeta_0) - \tfrac{1}{2}L_3(1-\zeta^2) \quad i=5,14$$
$$N_i = 2L_1L_2(1+\zeta_0) \quad i=2,11$$
$$N_i = 2L_2L_3(1+\zeta_0) \quad i=4,13$$
$$N_i = 2L_3L_1(1+\zeta_0) \quad i=6,15$$
$$N_7 = L_1(1-\zeta^2)$$
$$N_8 = L_2(1-\zeta^2)$$
$$N_9 = L_3(1-\zeta^2) \qquad (1.22)$$

where L_1 , L_2 and L_3 are area coordinates, with the relationship: $L_1 + L_2 + L_3 = 1$, and for each node, the value of (ξ, η, ζ) is listed as follows:

node	L_1	L_2	L_3	ζ
1	1	0	0	-1
2	0.5	0.5	0	-1
3	0	1	0	-1
4	0	0.5	0.5	-1
5	0	0	1	-1
6	0.5	0	0.5	-1
7	1	0	0	0
8	0	1	0	0
9	0	0	1	0
10	1	0	0	1
11	0.5	0.5	0	1
12	0	1	0	1
13	0	0.5	0.5	1
14	0	0	1	1
15	0.5	0	0.5	1

P516303 PDF [Page: 61 of 70]

APPENDIX 2 Effect of Complex Poisson's Ratio on Condensation Procedure

The following sections present the theory used in order to condense the resulting finite element matrices used to describe the behaviour of the isolators whose constitutive properties are such that both Young's Modulus and Poisson's Ratio can have both real and imaginary components to their moduli.

The general relationship between stress and strain within a viscoelastic medium can be expressed as

$$\sigma_{jk}(t) = G_{jklm}(0)\varepsilon_{lm}(t) + \int_0^t \varepsilon_{lm}(t-\tau)\frac{dG_{jklm}(\tau)}{d\tau}d\tau = G_{jklm} * d\varepsilon_{lm} \qquad (2.1)$$

where $\varepsilon_{lm} = \frac{1}{2}(u_{l,m} + u_{m,l})$.

$G_{jklm}(t)$ are known as the relaxation kernels for the material and * is used to denote the Stieltjes convolution. The number of independent relaxation kernels is dependent upon the anisotropic characteristics of the material. For an isotropic medium, there only are two kernels, $G_1(t)$ and $G_2(t)$:

$$G_{jklm}(t) = \tfrac{1}{3}(3G_2(t) - 2G_1(t))\delta_{jk}\delta_{lm} + G_1(t)(\delta_{jl}\delta_{km} + \delta_{jm}\delta_{kl}) \qquad (2.2)$$

and the viscoelastic constitutive equations can be written in terms of the deviatoric components of stress s_{jk} and strain e_{jk}:

$$s_{jk} = G_1 * de_{jk}$$
$$\sigma_{ll} = G_2 * d\varepsilon_{ll}$$

where:

$$s_{jk} = \sigma_{jk} - \tfrac{1}{3}\delta_{jk}\sigma_{ll} \qquad s_{ll} = 0$$
$$e_{jk} = \varepsilon_{jk} - \tfrac{1}{3}\delta_{jk}\varepsilon_{ll} \qquad e_{ll} = 0$$

If the response of the specimen is harmonic such that $\varepsilon_{jk}(t) = \varepsilon_{jk}\, e^{i\omega t}$, then

$$\sigma_{jk}(t) = G^*_{jklm}(i\omega)\varepsilon_{lm}\, e^{i\omega t} \qquad (2.3)$$

where $G^*_{jklm}(i\omega)$ are called the complex viscoelastic moduli.

There exist the following relations between $G_1^*(i\omega)$, $G_2^*(i\omega)$ and complex Young's modulus $E^*(i\omega)$, complex Poisson's ratio $\nu^*(i\omega)$:

$$E^*(i\omega) = \frac{9G_1^*(i\omega)G_2^*(i\omega)}{G_1^*(i\omega) + 3G_2^*(i\omega)} \qquad \nu^*(i\omega) = \frac{3G_2^*(i\omega) - 2G_1^*(i\omega)}{2G_1^*(i\omega) + 6G_2^*(i\omega)} \qquad (2.4)$$

or

$$G_1^*(i\omega) = \frac{E^*(i\omega)}{2(1+\nu^*(i\omega))} \qquad G_2^*(i\omega) = \frac{E^*(i\omega)}{3(1-2\nu^*(i\omega))} \qquad (2.5)$$

P516303 PDF [Page: 62 of 70]

$G_{jklm}(t)$ in Eq.(2.1) is usually called a relaxation function tensor of the viscoelastic material, and $G^*_{jklm}(i\omega)$ in Eq.(2.3) is a viscoelastic modulus tensor in the frequency domain. The ratio of the imaginary part to the real part is called the loss factor. A relaxation function that is commonly used is of an exponential form:

$$G_{jklm}(t) = G^{\infty}_{jklm} + \sum_{n=1}^{N_n} G^{(n)}_{jklm} e^{-b_n t} \tag{2.6}$$

and the corresponding viscoelastic modulus in the Laplace domain is:

$$G^*_{jklm}(s) = G^{\infty}_{jklm} + \sum_{n=1}^{N_n} G^{(n)}_{jklm} \frac{s}{s+b_n} \tag{2.7}$$

Modeling of Viscoelastic Mounts

The isolator can be assumed to be composed of a viscoelastic body with two elastic or rigid masses above and below. The following equation describes the deformation of the isolation mount:

$$\mathbf{M}\ddot{\mathbf{a}} + \mathbf{K}_e \mathbf{a} + \sum_{j=1}^{N_g} \mathbf{K}_{vj} G_j(t) * d\mathbf{a} = \mathbf{f} \tag{2.8}$$

$$\mathbf{M} = \begin{bmatrix} \mathbf{M}_{tt} & \mathbf{M}_{tc} & 0 & 0 & 0 \\ \mathbf{M}_{ct} & \mathbf{M}^t_{cc}+\mathbf{M}^t_{vv} & \mathbf{M}^t_{cv} & 0 & 0 \\ 0 & \mathbf{M}^t_{vc} & \mathbf{M}_{vv} & \mathbf{M}^b_{vc} & 0 \\ 0 & 0 & \mathbf{M}^b_{vc} & \mathbf{M}^b_{cc}+\mathbf{M}^b_{vv} & \mathbf{M}_{cb} \\ 0 & 0 & 0 & \mathbf{M}_{bc} & \mathbf{M}_{bb} \end{bmatrix} \qquad \mathbf{K}_e = \begin{bmatrix} \mathbf{K}_{tt} & \mathbf{K}_{tc} & 0 & 0 & 0 \\ \mathbf{K}_{ct} & \mathbf{K}^t_{cc} & 0 & 0 & 0 \\ 0 & 0 & 0 & 0 & 0 \\ 0 & 0 & 0 & \mathbf{K}^b_{cc} & \mathbf{K}_{cb} \\ 0 & 0 & 0 & \mathbf{K}_{bc} & \mathbf{K}_{bb} \end{bmatrix}$$

$$\mathbf{K}_{vj} = \begin{bmatrix} 0 & 0 & 0 & 0 & 0 \\ 0 & \mathbf{K}^t_{vv} & \mathbf{K}^t_{cv} & 0 & 0 \\ 0 & \mathbf{K}^t_{vc} & \mathbf{K}_{vv} & \mathbf{K}^b_{vc} & 0 \\ 0 & 0 & \mathbf{K}^b_{cv} & \mathbf{K}^b_{vv} & 0 \\ 0 & 0 & 0 & 0 & 0 \end{bmatrix}_j \qquad \mathbf{a} = \begin{bmatrix} \mathbf{a}_t^T & \mathbf{a}_{tc}^T & \mathbf{a}_v^T & \mathbf{a}_{bc}^T & \mathbf{a}_b^T \end{bmatrix}^T$$

$$\mathbf{f} = \begin{bmatrix} \hat{\mathbf{f}}_t^T & 0 & 0 & 0 & \hat{\mathbf{f}}_b^T \end{bmatrix}^T$$

where N_g is the number of independent viscoelastic kernels (2 for an isotropic material). The subscripts or superscripts t, b, v and c denotes the top mass, the base mass, the viscoelastic material domain and the connection boundary respectively. $\mathbf{a}_t$, $\mathbf{a}_b$, $\mathbf{a}_v$, $\mathbf{a}_{tc}$ and $\mathbf{a}_{bc}$ are vectors representing the displacements of top mass, base mass, isolator, connection points between top mass and the isolator, and connection points between base mass and the isolator respectively. It is assumed that each finite element node has three translational degrees of freedom. A bold letter represents a matrix or vector.

P516303.PDF [Page: 63 of 70]

Usually the top and bottom masses are tightly glued to the viscoelastic material. If the top and base masses are assumed rigid the displacement of every node located on the top and base masses can be represented in terms of two displacement vectors, one for each mass:

$$\mathbf{a}_{tj} = \mathbf{T}_t\,\mathbf{u}_t \qquad \mathbf{a}_{bj} = \mathbf{T}_b\,\mathbf{u}_b \tag{2.9}$$

where the matrix $\mathbf{T}_t$, $\mathbf{T}_b$ describes a rigid body transformation between the j node and the centroid of the top, bottom mass respectively.

Thus Eq. (2.8) can be written:

$$\begin{bmatrix} \mathbf{M}_{tt} & \mathbf{M}_{tv} & \mathbf{0} \\ \mathbf{M}_{vt} & \mathbf{M}_{vv} & \mathbf{M}_{vb} \\ \mathbf{0} & \mathbf{M}_{bv} & \mathbf{M}_{bb} \end{bmatrix} \begin{Bmatrix} \ddot{\mathbf{u}}_t \\ \ddot{\mathbf{a}}_v \\ \ddot{\mathbf{u}}_b \end{Bmatrix} + \sum_{j=1}^{N_g} \begin{bmatrix} \mathbf{K}_{tt} & \mathbf{K}_{tv} & \mathbf{0} \\ \mathbf{K}_{vt} & \mathbf{K}_{vv} & \mathbf{K}_{vb} \\ \mathbf{0} & \mathbf{K}_{bv} & \mathbf{K}_{bb} \end{bmatrix}_j G_j(t) * d \begin{Bmatrix} \mathbf{u}_t \\ \mathbf{a}_v \\ \mathbf{u}_b \end{Bmatrix} = \begin{Bmatrix} \mathbf{f}_t \\ \mathbf{0} \\ \mathbf{f}_b \end{Bmatrix} \tag{2.10}$$

The Solution Method for Complex Poisson's Ratio

For the complex Poisson's Ratio case, there are at least two complex functions in the dynamic equation of the isolators. Usually, the mass of isolator is very small compared with the engine mass, so it can be ignored. [This assumption however, also means that the analysis will not be able to predict local vibration modes in the isolators themselves. These are typically at much higher frequencies than the rigid body modes under consideration in the present study.]

The motion equation (2.10) after transferring it to the Laplace domain can be written as :

$$s^2 \begin{bmatrix} \mathbf{M}_{tt} & \mathbf{0} & \mathbf{0} \\ \mathbf{0} & \mathbf{0} & \mathbf{0} \\ \mathbf{0} & \mathbf{0} & \mathbf{M}_{bb} \end{bmatrix} \begin{Bmatrix} \bar{\mathbf{u}}_t \\ \bar{\mathbf{a}}_v \\ \bar{\mathbf{u}}_b \end{Bmatrix} + \sum_{j=1}^{N_g} \begin{bmatrix} \mathbf{K}_{tt} & \mathbf{K}_{tv} & \mathbf{0} \\ \mathbf{K}_{vt} & \mathbf{K}_{vv} & \mathbf{K}_{vb} \\ \mathbf{0} & \mathbf{K}_{bv} & \mathbf{K}_{bb} \end{bmatrix}_j G_j^*(s) \begin{Bmatrix} \bar{\mathbf{u}}_t \\ \bar{\mathbf{a}}_v \\ \bar{\mathbf{u}}_b \end{Bmatrix} = \begin{Bmatrix} \bar{\mathbf{f}}_t \\ \mathbf{0} \\ \bar{\mathbf{f}}_b \end{Bmatrix} \tag{2.11}$$

In order to reduce the number of degrees of freedom that need to be considered in the final analysis a condensation approach is adopted. For this case a so-called quasi-static condensation procedure will be used:

$$\bar{\mathbf{a}}_v = \mathbf{T}_t(s)\bar{\mathbf{u}}_t + \mathbf{T}_b(s)\bar{\mathbf{u}}_b \tag{2.12}$$

$$\mathbf{T}_t(s) = -[\sum_{j=1}^{N_g} \mathbf{K}_{vvj} G_j^*(s)]^{-1} \sum_{j=1}^{N_g} \mathbf{K}_{vtj} G_j^*(s) \tag{2.13}$$

$$\mathbf{T}_b(s) = -[\sum_{j=1}^{N_g} \mathbf{K}_{vvj} G_j^*(s)]^{-1} \sum_{j}^{N_g} \mathbf{K}_{vbj} G_j^*(s) \tag{2.14}$$

P516303 PDF [Page: 64 of 70]

When $N_g = 1$, the procedure reduces to the static condensation approach used for the elastic case:

$$\bar{\mathbf{s}}_v = -\mathbf{K}_{vv1}^{-1}[\mathbf{K}_{vt1}\bar{\mathbf{u}}_t + \mathbf{K}_{vb1}\bar{\mathbf{u}}_b] \tag{2.15}$$

After condensation, the governing equation (2.11) becomes

$$\begin{aligned}&\{s^2\begin{bmatrix}\mathbf{M}_{tt} & \mathbf{0}\\ \mathbf{0} & \mathbf{M}_{bb}\end{bmatrix} + \sum_{j=1}^{N_g}\begin{bmatrix}\mathbf{K}_{tt} & \mathbf{0}\\ \mathbf{0} & \mathbf{K}_{bb}\end{bmatrix}_j G_j^*(s)\\ &\quad + \begin{bmatrix}[\sum_{j=1}^{N_g}\mathbf{K}_{tvj}G_j^*(s)]\mathbf{T}_t(s) & [\sum_{j=1}^{N_g}\mathbf{K}_{tvj}G_j^*(s)]\mathbf{T}_b(s)\\ [\sum_{j=1}^{N_g}\mathbf{K}_{bvj}G_j^*(s)]\mathbf{T}_t(s) & [\sum_{j=1}^{N_g}\mathbf{K}_{bvj}G_j^*(s)]\mathbf{T}_b(s)\end{bmatrix}\begin{Bmatrix}\bar{\mathbf{u}}_t\\ \bar{\mathbf{u}}_b\end{Bmatrix} = \begin{Bmatrix}\bar{\mathbf{f}}_t\\ \bar{\mathbf{f}}_b\end{Bmatrix}\end{aligned} \tag{2.16}$$

For an isotropic material, the complex moduli can be rewritten as

$$G_j^*(s) = E^*(s)g_j(\nu^*(s)) = E^*(s)[g_j(\nu^*(0)) + q_j(s)] \tag{2.17}$$

in which $q_j(s)$ represents the difference between the complex and the real Poisson's ratio, and is given by

$$q_j(s) = g_j(\nu^*(s)) - g_j(\nu^*(0)) \tag{2.18}$$

where $q_j(0) = 0$.

Then, expanding the last term of Eq.(2.16) as a power series of $q_j(s)$:

$$\begin{aligned}\left[\sum_{j=1}^{N_g}\mathbf{K}_{vvj}G_j^*(s)\right]^{-1} &= \left[E^*(s)\left\{\mathbf{K}_{vv0} + \sum_{j=1}^{N_g}\mathbf{K}_{vvj}q_j(s)\right\}\right]^{-1}\\ &= \left[E^*(s)\mathbf{K}_{vv0}\left\{\mathbf{I} + \sum_{j=1}^{N_g}\tilde{\mathbf{K}}_{vvj}q_j(s)\right\}\right]^{-1} = E^*(s)^{-1}\left[\mathbf{I} + \sum_{j=1}^{N_g}\tilde{\mathbf{K}}_{vvj}q_j(s)\right]^{-1}\mathbf{K}_{vv0}^{-1}\end{aligned} \quad 2.19$$

$$= E^*(s)^{-1}\left[\mathbf{I} - \sum_{j=1}^{N_g}\tilde{\mathbf{K}}_{vvj}q_j(s) + \sum_{j=1}^{N_g}\tilde{\mathbf{K}}_{vvj}\sum_{l=1}^{N_g}\tilde{\mathbf{K}}_{vvl}q_j(s)q_l(s) + \cdots\right]\mathbf{K}_{vv0}^{-1}$$

$$\sum_{j=1}^{N_g}\mathbf{K}_{nvj}G_j^*(s) = E^*(s)\left[\mathbf{K}_{nv0} + \sum_{j=1}^{N_g}\mathbf{K}_{nvj}q_j(s)\right] \tag{2.20}$$

where $\mathbf{K}_{nv0} = \sum_{j=1}^{N_g}\mathbf{K}_{nvj}g_j(\nu^*(0))$, $\tilde{\mathbf{K}}_{vvj} = \mathbf{K}_{vv0}^{-1}\mathbf{K}_{vvj}$, and $\mathbf{n} = \mathbf{t}, \mathbf{v}$

And

P516303.PDF [Page: 65 of 70]

$$\begin{bmatrix}\sum_{j=1}^{N_g}\mathbf{K}_{tvj}G_j^*(s)\\ \sum_{j=1}^{N_g}\mathbf{K}_{bvj}G_j^*(s)\end{bmatrix}\left[\sum_{j=1}^{N_g}\mathbf{K}_{vvj}G_j^*(s)\right]^{-1}\begin{bmatrix}\sum_{j=1}^{N_g}\mathbf{K}_{vtj}{}^TG_j^*(s)\\ \sum_{j=1}^{N_g}\mathbf{K}_{vbj}{}^TG_j^*(s)\end{bmatrix}^T$$

$$\doteq\begin{bmatrix}\mathbf{K}_{tv0}+\sum_{j=1}^{N_g}\mathbf{K}_{tvj}q_j(s)\\ \mathbf{K}_{bv0}+\sum_{j=1}^{N_g}\mathbf{K}_{bvj}q_j(s)\end{bmatrix}\mathbf{K}_{vv0}{}^{-1}\begin{bmatrix}\mathbf{K}_{vt0}{}^T+\sum_{j=1}^{N_g}\mathbf{K}_{vtj}{}^Tq_j(s)\\ \mathbf{K}_{vb0}{}^T+\sum_{j=1}^{N_g}\mathbf{K}_{vbj}{}^Tq_j(s)\end{bmatrix}^T$$

$$-\begin{bmatrix}\mathbf{K}_{tv0}+\sum_{j=1}^{N_g}\mathbf{K}_{tvj}q_j(s)\\ \mathbf{K}_{bv0}+\sum_{j=1}^{N_g}\mathbf{K}_{bvj}q_j(s)\end{bmatrix}\sum_{j=1}^{N_g}\tilde{\mathbf{K}}_{vvj}q_j(s)\mathbf{K}_{vv0}{}^{-1}\begin{bmatrix}\mathbf{K}_{vt0}{}^T+\sum_{j=1}^{N_g}\mathbf{K}_{vtj}{}^Tq_j(s)\\ \mathbf{K}_{vb0}{}^T+\sum_{j=1}^{N_g}\mathbf{K}_{vbj}{}^Tq_j(s)\end{bmatrix}^T$$

$$+\begin{bmatrix}\mathbf{K}_{tv0}\\ \mathbf{K}_{bv0}\end{bmatrix}\sum_{j=1}^{N_g}\tilde{\mathbf{K}}_{vvj}\sum_{l=1}^{N_g}\tilde{\mathbf{K}}_{vvl}q_j(s)q_l(s)\mathbf{K}_{vv0}{}^{-1}\begin{bmatrix}\mathbf{K}_{vt0}{}^T\\ \mathbf{K}_{vb0}{}^T\end{bmatrix}^T$$

$$=\frac{1}{2}\begin{bmatrix}\sum_{j=1}^{N_g}\mathbf{K}_{tvj}G_j^*(s)\\ \sum_{j=1}^{N_g}\mathbf{K}_{bvj}G_j^*(s)\end{bmatrix}\mathbf{K}_{vv0}{}^{-1}\begin{bmatrix}\mathbf{K}_{vt0}{}^T\\ \mathbf{K}_{vb0}{}^T\end{bmatrix}^T+\frac{1}{2}\begin{bmatrix}\mathbf{K}_{tv0}\\ \mathbf{K}_{bv0}\end{bmatrix}\mathbf{K}_{vv0}{}^{-1}\begin{bmatrix}\sum_{j=1}^{N_g}\mathbf{K}_{vtj}{}^TG_j^*(s)\\ \sum_{j=1}^{N_g}\mathbf{K}_{vbj}{}^TG_j^*(s)\end{bmatrix}$$

$$+\frac{1}{2}\begin{bmatrix}\sum_{j=1}^{N_g}\mathbf{K}_{tvj}G_j^*(s)\\ \sum_{j=1}^{N_g}\mathbf{K}_{bvj}G_j^*(s)\end{bmatrix}\mathbf{K}_{vv0}{}^{-1}\begin{bmatrix}\sum_{j=1}^{N_g}\mathbf{K}_{vtj}{}^Tq_j(s)\\ \sum_{j=1}^{N_g}\mathbf{K}_{vbj}{}^Tq_j(s)\end{bmatrix}^T+\frac{1}{2}\begin{bmatrix}\sum_{j=1}^{N_g}\mathbf{K}_{tvj}q_j(s)\\ \sum_{j=1}^{N_g}\mathbf{K}_{bvj}q_j(s)\end{bmatrix}\mathbf{K}_{vv0}{}^{-1}\begin{bmatrix}\sum_{j=1}^{N_g}\mathbf{K}_{vtj}{}^TG_j^*(s)\\ \sum_{j=1}^{N_g}\mathbf{K}_{vbj}{}^TG_j^*(s)\end{bmatrix}$$

$$-\begin{bmatrix}\mathbf{K}_{tv0}+\sum_{j=1}^{N_g}\mathbf{K}_{tvj}q_j(s)\\ \mathbf{K}_{bv0}+\sum_{j=1}^{N_g}\mathbf{K}_{bvj}q_j(s)\end{bmatrix}\sum_{j=1}^{N_g}\tilde{\mathbf{K}}_{vvj}q_j(s)\mathbf{K}_{vv0}{}^{-1}\begin{bmatrix}\mathbf{K}_{vt0}{}^T+\sum_{j=1}^{N_g}\mathbf{K}_{vtj}{}^Tq_j(s)\\ \mathbf{K}_{vb0}{}^T+\sum_{j=1}^{N_g}\mathbf{K}_{vbj}{}^Tq_j(s)\end{bmatrix}^T$$

$$+\begin{bmatrix}\mathbf{K}_{tv0}\\ \mathbf{K}_{bv0}\end{bmatrix}\sum_{j=1}^{N_g}\tilde{\mathbf{K}}_{vvj}\sum_{l=1}^{N_g}\tilde{\mathbf{K}}_{vvl}q_j(s)q_l(s)\mathbf{K}_{vv0}{}^{-1}\begin{bmatrix}\mathbf{K}_{vt0}{}^T\\ \mathbf{K}_{vb0}{}^T\end{bmatrix}^T$$

The above equation is (2.21).

The governing equation (2.16) then becomes:

P516303.PDF [Page: 66 of 70]

$$\left[s^2 \begin{bmatrix} \mathbf{M}_{tt} & \mathbf{0} \\ \mathbf{0} & \mathbf{M}_{bb} \end{bmatrix} + \sum_{j=1}^{N_g} \begin{bmatrix} \tilde{\mathbf{K}}_{tt} & \tilde{\mathbf{K}}_{tb} \\ \tilde{\mathbf{K}}_{bt} & \tilde{\mathbf{K}}_{bb} \end{bmatrix}_j G_j^*(s) + \begin{bmatrix} \hat{\mathbf{K}}_{tt} & \hat{\mathbf{K}}_{tb} \\ \hat{\mathbf{K}}_{bt} & \hat{\mathbf{K}}_{bb} \end{bmatrix} E^*(s) \right] \begin{Bmatrix} \bar{\mathbf{u}}_t \\ \bar{\mathbf{u}}_b \end{Bmatrix} = \begin{Bmatrix} \bar{\mathbf{f}}_t \\ \bar{\mathbf{f}}_b \end{Bmatrix} \tag{2.22}$$

in which:

$$\tilde{\mathbf{K}}_{tt_j} = \mathbf{K}_{tt_j} + \tfrac{1}{2}\mathbf{K}_{tv_j}\mathbf{K}_{vv0}^{-1}\mathbf{K}_{vt0} + \tfrac{1}{2}\mathbf{K}_{tv0}\mathbf{K}_{vv0}^{-1}\mathbf{K}_{vt_j}$$

$$\tilde{\mathbf{K}}_{tb_j} = \mathbf{K}_{tb_j} + \tfrac{1}{2}\mathbf{K}_{tv_j}\mathbf{K}_{vv0}^{-1}\mathbf{K}_{vb0} + \tfrac{1}{2}\mathbf{K}_{tv0}\mathbf{K}_{vv0}^{-1}\mathbf{K}_{vb_j}$$

$$\tilde{\mathbf{K}}_{bt_j} = \tilde{\mathbf{K}}_{tb_j}^{T}$$

$$\tilde{\mathbf{K}}_{bb_j} = \mathbf{K}_{bb_j} + \tfrac{1}{2}\mathbf{K}_{bv_j}\mathbf{K}_{vv0}^{-1}\mathbf{K}_{vb0} + \tfrac{1}{2}\mathbf{K}_{bv0}\mathbf{K}_{vv0}^{-1}\mathbf{K}_{vb_j}$$

When $N_g = 1$, $q_1(s) = 0$, and the last term of Eq (2.22) vanishes, and

$$\left[s^2 \begin{bmatrix} \mathbf{M}_{tt} & \mathbf{0} \\ \mathbf{0} & \mathbf{M}_{bb} \end{bmatrix} + E^*(s) \begin{bmatrix} \tilde{\mathbf{K}}_{tt} & \tilde{\mathbf{K}}_{tb} \\ \tilde{\mathbf{K}}_{bt} & \tilde{\mathbf{K}}_{bb} \end{bmatrix} \right] \begin{Bmatrix} \bar{\mathbf{u}}_t \\ \bar{\mathbf{u}}_b \end{Bmatrix} = \begin{Bmatrix} \bar{\mathbf{f}}_t \\ \bar{\mathbf{f}}_b \end{Bmatrix} \tag{2.23}$$

$$\tilde{\mathbf{K}}_{tt} = \mathbf{K}_{tt0} + \mathbf{K}_{tv0}\mathbf{K}_{vv0}^{-1}\mathbf{K}_{vt0}$$

$$\tilde{\mathbf{K}}_{tb} = \mathbf{K}_{tb0} + \mathbf{K}_{tv0}\mathbf{K}_{vv0}^{-1}\mathbf{K}_{vb0}$$

$$\tilde{\mathbf{K}}_{bt} = \tilde{\mathbf{K}}_{tb}^{T}$$

$$\tilde{\mathbf{K}}_{bb} = \mathbf{K}_{bb0} + \mathbf{K}_{bv0}\mathbf{K}_{vv0}^{-1}\mathbf{K}_{vb0}$$

which corresponds to the case of real Poisson's ratio.
The last term of the governing equation (2.22) is composed of two parts

$$\hat{\mathbf{K}} = \sum_{j=1}^{N_g} \mathbf{K}_{q_j} \mathbf{q}_j(s) + \sum_{j=1}^{N_g} \sum_{l=1}^{N_g} \mathbf{K}_{qq_{jl}} \mathbf{q}_j(s) \mathbf{q}_l(s) \tag{2.24}$$

where

$$\mathbf{K}_{q_j} = \frac{1}{2}\begin{bmatrix} \mathbf{K}_{tv0} \\ \mathbf{K}_{bv0} \end{bmatrix} \mathbf{K}_{vv0}^{-1} \begin{bmatrix} \mathbf{K}_{vt_j}^{T} \\ \mathbf{K}_{vb_j}^{T} \end{bmatrix}^{T} + \frac{1}{2}\begin{bmatrix} \mathbf{K}_{tv_j} \\ \mathbf{K}_{bv_j} \end{bmatrix} \mathbf{K}_{vv0}^{-1} \begin{bmatrix} \mathbf{K}_{vt0}^{T} \\ \mathbf{K}_{vb0}^{T} \end{bmatrix}^{T} - \begin{bmatrix} \mathbf{K}_{tv0} \\ \mathbf{K}_{bv0} \end{bmatrix} \tilde{\mathbf{K}}_{vv_j} \mathbf{K}_{vv0}^{-1} \begin{bmatrix} \mathbf{K}_{vt0}^{T} \\ \mathbf{K}_{vb0}^{T} \end{bmatrix}^{T} \tag{2.25}$$

$$\mathbf{K}_{qq_{jl}} = \begin{bmatrix} \mathbf{K}_{tv_j} \\ \mathbf{K}_{bv_j} \end{bmatrix} \mathbf{K}_{vv0}^{-1} \begin{bmatrix} \mathbf{K}_{vt_l}^{T} \\ \mathbf{K}_{vb_l}^{T} \end{bmatrix}^{T} - \begin{bmatrix} \mathbf{K}_{tv_j} \\ \mathbf{K}_{bv_j} \end{bmatrix} \tilde{\mathbf{K}}_{vv_l} \mathbf{K}_{vv0}^{-1} \begin{bmatrix} \mathbf{K}_{vt0}^{T} \\ \mathbf{K}_{vb0}^{T} \end{bmatrix}^{T} - \begin{bmatrix} \mathbf{K}_{tv0} \\ \mathbf{K}_{bv0} \end{bmatrix} \tilde{\mathbf{K}}_{vv_j} \mathbf{K}_{vv0}^{-1} \begin{bmatrix} \mathbf{K}_{vt_l}^{T} \\ \mathbf{K}_{vb_l}^{T} \end{bmatrix}^{T} + \begin{bmatrix} \mathbf{K}_{tv0} \\ \mathbf{K}_{bv0} \end{bmatrix} \tilde{\mathbf{K}}_{vv_j} \tilde{\mathbf{K}}_{vv_l} \mathbf{K}_{vv0}^{-1} \begin{bmatrix} \mathbf{K}_{vt0}^{T} \\ \mathbf{K}_{vb0}^{T} \end{bmatrix}^{T} \tag{2.26}$$

Retaining only the first part of $\hat{\mathbf{K}}$, equation (2.22) can then be easily transferred back to time domain. From eq.(2.18):

P516303.PDF [Page: 67 of 70]

$$E^*(s)q_j(s) = G_j^*(s) - E^*(s)g_j(v^*(0))$$

Thus the governing equation after condensation will be

$$\begin{bmatrix} \mathbf{M}_{tt} & \mathbf{0} \\ \mathbf{0} & \mathbf{M}_{bb} \end{bmatrix} \begin{Bmatrix} \ddot{\mathbf{u}}_t \\ \ddot{\mathbf{u}}_b \end{Bmatrix} + \sum_{j=1}^{N_d} \begin{bmatrix} \tilde{\mathbf{K}}_{tt} & \tilde{\mathbf{K}}_{tb} \\ \tilde{\mathbf{K}}_{bt} & \tilde{\mathbf{K}}_{bb} \end{bmatrix}_j G_j(t) * d \begin{Bmatrix} \mathbf{u}_t \\ \mathbf{u}_b \end{Bmatrix} + \sum_{j=1}^{N_d} \mathbf{K}_{tb} [G_j(t) - E(t)g_j(v^*(0))] * d \begin{Bmatrix} \mathbf{u}_t \\ \mathbf{u}_b \end{Bmatrix} = \begin{Bmatrix} \mathbf{f}_t \\ \mathbf{f}_b \end{Bmatrix} \tag{2.27}$$

UNCLASSIFIED
SECURITY CLASSIFICATION OF FORM
(highest classification of Title, Abstract, Keywords)

DOCUMENT CONTROL DATA

(Security classification of title, body of abstract and indexing annotation must be entered when the overall document is classified)

1. ORIGINATOR (the name and address of the organization preparing the document. Organizations for whom the document was prepared, e.g. Establishment sponsoring a contractor's report, or tasking agency, are entered in section 8)

Vibe-Tek Research Ltd
5662 Holland St, Vancouver, BC, V6N 2A8

2. SECURITY CLASSIFICATION (overall security classification of the document including special warning terms if applicable)

UNCLASSIFIED

3 TITLE (the complete document title as indicated on the title page. Its classification should be indicated by the appropriate abbreviation (S,C,R or U) in parentheses after the title).

Optimization of Vibration Mount Properties for Application to Shipboard Diesel Engines- Phase III

4 AUTHORS (Last name, first name, middle initial. If military, show rank, e.g. Doe, Maj. John E.)

Hutton S.G

5. DATE OF PUBLICATION (month and year of publication of document)	6a. NO .OF PAGES (total containing information Include Annexes, Appendices, etc).	6b NO OF REFS (total cited in document)
January 2001	63	5

7 DESCRIPTIVE NOTES (the category of the document, e.g. technical report, technical note or memorandum. If appropriate, enter the type of report, e.g. interim, progress, summary, annual or final. Give the inclusive dates when a specific reporting period is covered)

CONTRACTOR REPORT

8 SPONSORING ACTIVITY (the name of the department project office or laboratory sponsoring the research and development Include address)

Defence Research Establishment Atlantic
PO Box 1012
Dartmouth, NS, Canada B2Y 3Z7

9a PROJECT OR GRANT NO (if appropriate, the applicable research and development project or grant number under which the document was written. Please specify whether project or grant).	9b CONTRACT NO (if appropriate, the applicable number under which the document was written)
Project 1gc12, 1gh14, and 1ga23	W7707-9-7025/001/HAL,W7707-9-7293/001/HAL

10a ORIGINATOR'S DOCUMENT NUMBER (the official document number by which the document is identified by the originating activity This number must be unique to this document)	10b OTHER DOCUMENT NOs. (Any other numbers which may be assigned this document either by the originator or by the sponsor)
none	DREA CR 2000-077

11 DOCUMENT AVAILABILITY (any limitations on further dissemination of the document, other than those imposed by security classification)

(X) Unlimited distribution
( ) Defence departments and defence contractors; further distribution only as approved
( ) Defence departments and Canadian defence contractors; further distribution only as approved
( ) Government departments and agencies; further distribution only as approved
( ) Defence departments; further distribution only as approved
( ) Other (please specify):

12 DOCUMENT ANNOUNCEMENT (any limitation to the bibliographic announcement of this document. This will normally correspond to the Document Availability (11) However, where further distribution (beyond the audience specified in (11) is possible, a wider announcement audience may be selected)

Unlimited

UNCLASSIFIED
SECURITY CLASSIFICATION OF FORM

P516303.PDF [Page: 69 of 70]

13. ABSTRACT (a brief and factual summary of the document. It may also appear elsewhere in the body of the document itself. It is highly desirable that the abstract of classified documents be unclassified. Each paragraph of the abstract shall begin with an indication of the security classification of the information in the paragraph (unless the document itself is unclassified) represented as (S), (C), (R), or (U). It is not necessary to include here abstracts in both official languages unless the text is bilingual).

This report describes the theory and capabilities of MATLAB programs that have been developed in order to assist in the optimal vibration design of isolators for marine engines. These programs calculate the vibration transmissibility characteristics of the system and are of value in the design of optimal isolation systems. A program is also developed for the analysis of the active control of transmitted vibrations. The frequency range of interest is that encompassing the natural frequencies of the engine on its support system. The general system that is analysed consists of an engine supported by vibration isolators on a foundation raft that itself is supported to ground by vibration isolators. The programs model the engine as a rigid body. The foundation raft can be modeled as a rigid body, or it can be modeled as a flexible body using beam finite elements. It is assumed that the isolators can be modeled as an isotropic linear viscoelastic material in terms of both a complex Young's modulus and a complex Poisson's Ratio, both of which are frequency dependant. The report describes three different approaches to the modeling of the isolators: i) an approach based upon finite element analysis of the viscoelastic isolators using constitutive data of the isolator material; ii) an approach based upon the results of dynamic stiffness measurements conducted on engine mounts; and iii) an approach based upon the results of so called 4-pole parameter data that describes the velocity force transfer matrices measured on full sized mounts in a given direction. In both the cases that involve experimentally determined isolator characteristics the data measured is not likely to completely describe the isolator characteristics. In such cases the programs developed have utilized an analytical approach to provide the missing data. Numerical results are presented to illustrate each of the approaches developed. The report also contains the development of an active control option which is used to evaluate the potential for active control to be used in order to minimise the levels of force transmitted from the engine to the support.

14. KEYWORDS, DESCRIPTORS or IDENTIFIERS (technically meaningful terms or short phrases that characterize a document and could be helpful in cataloguing the document. They should be selected so that no security classification is required. Identifiers, such as equipment model designation, trade name, military project code name, geographic location may also be included. If possible keywords should be selected from a published thesaurus. e.g. Thesaurus of Engineering and Scientific Terms (TEST) and that thesaurus-identified. If it not possible to select indexing terms which are Unclassified, the classification of each should be indicated as with the title)

diesel engine vibration
vibration isolation
resilient suspension
visco elasticity
active vibration control

DCD03 2/06/87-M/ DREA mod 17 Dec 1997